Soluble Corn Fiber Consumption Effects Executive Functions and Gut Microbiota in Middle to Older Age Adults: A Randomized Controlled Crossover Trial

*David A. Alvarado[1,4], *Tori A. Holthaus[1], Shelby Martell[2], Nicole L. Southey[1], Marco Atallah[4], Rhea Sarma[3], David Revilla[4], Marina Brown[4], Twinkle Mehta[3], Naiman A. Khan[1,2,3,5], Hannah D. Holscher[1,4]

[1]Division of Nutritional Sciences, University of Illinois, Urbana-Champaign, Urbana, IL 61801, USA
[2]Neuroscience Program, University of Illinois, Urbana-Champaign, Urbana, IL 61801, USA
[3]Health and Kinesiology, University of Illinois, Urbana-Champaign, Urbana, IL 61801, USA
[4]Department of Food Science and Human Nutrition, University of Illinois, Urbana-Champaign, Urbana, IL 61801, USA
[5]Beckman Institute of Advanced Science and Technology, Urbana-Champaign, Urbana, IL 61801, USA

*Shared first-authorship

Sources of Support: This work was supported by Tate & Lyle Ingredients Americas LLC and the USDA NIFA, Hatch Project (1026591, to HDH).

Clinical Trial Registry: NCT05066425

Corresponding Author: Hannah D. Holscher, 1201 West Gregory Drive Urbana, IL 61801, (217) 300-2512, hholsche@illinois.edu

Data described in the manuscript, code book, and analytic code will be made available upon request.

Abbreviations: Soluble corn fiber (SCF, PROMITOR® Soluble Fibre™), Maltodextrin (CON, control), *Parabacteroides distasonis* (*Pd*), Short-chain Fatty-acids (SCFA), Event-related potential (ERP), Reaction Time (RT), Positive and Negative Affect Schedule (PANAS), Perceived Stress Score (PSS), carbohydrate-active (CA), Profile of Moods (POMS), Cambridge Neuropsychological Test Automated Battery (CANTAB), SE (Standard Error), SEM (Standard Error of the Mean), Std (Standardized)

Abstract

Background: Adequate dietary fiber may improve cognitive function through gut microbiota-mediated mechanisms, but human trials remain limited.

Objectives: This study evaluated the effects of soluble corn fiber (SCF) on cognition, gastrointestinal microbiota composition, and fermentation end-products, with pre-defined aims to investigate gastrointestinal microbiota-dependent mechanisms by which SCF consumption may underpin cognitive performance.

Methods: This randomized, double-blind, crossover trial included 42 healthy adults (45-75 yr) asked to consume maltodextrin (CON, 22 g/d) or SCF (22g/d; 18g/d fiber) for 4 weeks, separated by a 4-week washout in a counterbalanced order. Outcome assessments included cognitive control via the flanker task (with event-related potentials), Cambridge Neuropsychological Test Automated Battery (CANTAB), Profile of Moods Survey (POMS), and relational memory tasks; fecal microbiota via 16S rRNA and shotgun sequencing, targeted metabolomics via GC-MS; and self-reported subjective GI tolerance symptoms via daily questionnaires. *In vitro* and genomic analyses characterized microbial species and genes facilitating SCF fermentation.

Results: SCF consumption improved reaction times (RT) for congruent (P=0.03) and incongruent (P=0.002) task conditions of the flanker task compared to CON. Faster congruent RT was correlated with greater fecal concentrations of acetate (ρ= -0.33, P=0.048) and propionate (ρ= -0.36, P=0.03). *Parabacteroides* abundance was enriched with SCF (FDR P<0.001) and correlated with fecal acetate (ρ = 0.34, P=0.04) concentrations. Mediation analyses revealed no significant indirect effects; however, moderation analyses showed that the abundance of *Parabacteroides* moderated the effect of treatment on RT (P=0.03). Fecal metagenomic profiles from microbial responder identified *P. distasonis* (*Pd*) as the primary

species enriched from SCF consumption. *In vitro* culturing of *Pd* exhibited diauxic growth on SCF, characterized by an initial non-fiber sugar utilization phase (0-4 hrs), a lag phase (4-6 hrs), and a subsequent fiber fermentation phase (6-10 hrs), confirming its direct utilization of SCF. The predicted metagenome suggests SCF-enriched KEGG carbohydrate metabolism pathways (FDR $P < 0.05$), including carbohydrate-active (CA) KOs (FDR $P < 0.05$).

Conclusion: SCF consumption improved attentional inhibition and increased *Parabacteroides* abundance. Correlation analyses indicated higher *Parabacteroides* abundance were associated with increased fecal acetate, and fecal acetate was correlated with quicker congruent RTs. While no mediation was observed, *Parabacteroides* significantly moderated cognitive benefits, supporting the relevance of microbiota composition in shaping dietary fiber responsiveness in older adults.

Keywords: Reaction time, Attentional inhibition, Parabacteroides, gut-brain axis, cognitive control

Introduction

Converging evidence increasingly demonstrates the benefits of certain nutrients and overall diet quality to cognitive health and brain function[1–3]. Preclinical models have shown that high-fiber diets can improve cognitive function[4,5], yet human intervention studies remain scarce[6–8]. While much is known about the influence of dietary fiber on the gut microbiota, fewer studies have examined its impact on human cognitive function[9–11], and fewer still have explored the gut-microbiota-brain axis in rigorously controlled trials. These gaps highlight the need for clinical research evaluating whether fermentable fibers can influence cognition through gut microbiota-mediated mechanisms.

Resistant maltodextrins, such as soluble corn fiber (SCF), have physiological health benefits, including glycemic control, calcium and bone retention, and gastrointestinal health[9–11]. SCF is a non-viscous, water-soluble fiber with an average degree of polymerization (DP) between 10-12[12]. Due to its structural complexity, < 30% of SCF is digested in the small intestine, allowing it to reach the colon to be fermented by resident microbes[13,14]. SCF promotes the growth of commensal taxa, such as *Bifidobacterium*, *Lactobacillus,* and *Parabacteroides*[15,16], and increases short-chain fatty acid (SCFA) production across age groups[17]. These microbiota and metabolite shifts are potential pathways through which SCF could influence cognitive function, particularly via gut-brain signaling[18,21–24].

Cognitive functioning is supported by several executive processes, including inhibitory control, which enables individuals to suppress automatic responses in favor of goal-relevant behavior[18]. This form of top-down regulation is fundamental to attentional focus, working memory, and behavioral flexibility and is often assessed through tasks that require resolving conflicting information or suppressing irrelevant stimuli[18]. In addition to behavioral performance

72 measures such as accuracy (ACC) and reaction time (RT), neural markers of cognitive control
73 can be captured using event-related potentials (ERP) derived from electroencephalographic
74 (EEG) activity[19,20]. Given the growing evidence that microbial metabolites can influence brain
75 signaling and cognitive performance[21–26], examining both behavioral and neuroelectrical markers
76 provides a comprehensive evaluation of SCF's potential cognitive effects[26,27,33].
77 This study aimed to assess the effects of SCF consumption on behavioral measures of
78 cognitive functions among middle- and older-aged adults. For our primary aim, we hypothesized
79 that daily SCF consumption over four weeks would improve cognitive control and hippocampal-
80 dependent relational memory compared to placebo control. Furthermore, we aimed to examine
81 the impact of SCF consumption on neuroelectric indices of inhibitory control, hypothesizing that
82 SCF would improve neural efficiency. Secondary aims include assessing the effects of SCF
83 consumption on fecal microbiota and fermentation end-products. Finally, pre-determined tertiary
84 aims were to investigate whether cognitive improvements are mediated or moderated by
85 microbial and microbial metabolite changes.
86

87 **Methods**

88 *Study design and intervention*

89 This study used a double-blind, randomized, placebo-controlled, repeated measures
90 crossover design with two conditions (2x2 Latin square design). The intervention periods lasted
91 four weeks each, with a minimum two-week washout period between the conditions. Participants
92 were asked to consume 22 g/day of SCF (PROMITOR® Soluble Fibre™) containing 18g of SCF
93 or 22 g/day of maltodextrin (CON) during the respective intervention conditions. The two
94 supplements were identical in taste and appearance and were provided by Tate & Lyle in pre-

95 measured sachets of powder marked with a numerical identifier only to maintain the blindness of
96 the researchers and participants. All participants and research staff were blinded until data
97 analyses were completed. Since previous research has not directly examined the effects of SCF
98 consumption on cognitive function, we relied on a conservative approach, estimating a small
99 effect size. Based on an *a priori* power calculation (G-Power 3.1.9.2) [27] using an α of 0.05, β of
100 0.80, and a small effect size ($r = 0.20$), we determined that a total sample size of 36 participants
101 would be sufficient to conduct these analyses.

102 Participants were given 35 powder sachets per intervention period and were instructed to
103 mix one sachet of the powdered supplement into a liquid of their choice once daily for four
104 weeks. Participants were given a paper-based compliance log to track daily supplement intake
105 during each intervention period and were asked to return the log and any remaining sachets at the
106 end of each period for compliance tracking. Participants completed two in-person baseline
107 testing appointments before supplement deployment. Demographic and medical history were
108 collected via survey, including age, sex, approximate annual income, highest education level,
109 race, and ethnicity. Anthropometric measures and a cognitive battery were administered before
110 and after each intervention period. Participants performed cognitive testing during the first and
111 second baseline visits to minimize practice effects, and the cognitive tasks were presented in a
112 counterbalanced order at each visit using a Latin square design to avoid fatigue and order effects.
113 The study visits (**Supplemental Figure 1**) were conducted at the University of Illinois.
114

115 *Participants criteria*

116 Adults aged 45-75 years were recruited from the East Central Illinois area using popular
117 email newsletters, social media postings, community event displays via the postal service, and

118 flyers posted on public transport. Participants were excluded if they reported a previous
119 physician diagnosis of gastrointestinal or metabolic disease, including inflammatory bowel
120 disease and diabetes, had a prior diagnosis of any neurological disease, including dementia,
121 Parkinson's disease, multiple sclerosis, brain tumors, or autism, had colorblindness or vision not
122 corrected to 20/20, had antibiotic use within the last month, tobacco use, food allergies, and if
123 they were pregnant or lactating.

124 The study was registered on ClinicalTrials.gov (clinicaltrials.gov/study/NCT05066425),
125 approved by the University of Illinois Institutional Review Board, and conducted following the
126 principles of the Declaration of Helsinki. Participants were informed of all procedures, and their
127 written informed consent to the study procedures was obtained before data collection. Following
128 informed consent, participants were screened in person and excluded if their BMI was <18.5 or
129 >34.9 kg/m^2, if they had cognitive impairment as evidenced by a score of less than 24 on the
130 Mini-Mental State Examination, and if their intake of dietary fiber was > 70% of the Daily
131 Recommended Intake for fiber (≥18 g fiber per day for women and ≥27 g fiber per day for men)
132 according to the results of their completed Dietary History Questionnaire version 3 (DHQ3) food
133 frequency questionnaire. Eligible participants were then invited to complete further testing and
134 were asked to refrain from taking other probiotic or nutrition supplements and keep their dietary
135 intake and physical activity consistent for the duration of the study.

136 If participants were recruited and passed screening tests, they were randomized to start in
137 a counterbalanced order in either the SCF or CON group (**Table 1**) and assigned a study id (e.g.-
138 SC101) inputted onto REDCap by a trained member of the team. The Study Coordinator
139 generated the sequence of interventions assigned using a simple randomization approach (coin

toss) for each enrolled participant. Participants were given sachets labeled as 030 or 789, CON and SCF, respectively, to ensure double blinding throughout the study until completion.

Weight Status

For each visit, the participant's height and weight were measured in light clothing and without shoes using a SECA stadiometer (model 240; SECA, Hamburg, Germany) and Tanita WB-300 Plus digital scale (Tanita, Tokyo, Japan). Height and weight were taken in triplicate, and the average was used to calculate BMI using the formula weight [kg]/height [m^2].

Flanker task

Attentional inhibition was assessed using a modified Eriksen flanker task as previously described [28]. Briefly, participants were asked to respond (Current Designs, Philadelphia, PA, USA) quickly and accurately to the directionality of a central stimulus (3-cm tall white arrow) presented with two flanking stimuli on each side (83s stimulus presentation and 100ms response window, and jittered intertrial intervals of 1100, 1200, and 1500 ms). During congruent trials, the flanking arrows faced the same direction as the central arrow (i.e., <<<<<, >>>>>). During incongruent trials, the flanking arrows face the opposite direction of the central stimuli (i.e., >><>>, <<><<), requiring greater upregulation of attentional inhibition. The task began with 40 practice trials followed by two blocks of 200 randomized experimental trials. Behavioral measures of interest included accuracy (ACC) and reaction time (RT) for correct responses during congruent and incongruent trials. The interference effect (flanker effect) for ACC was also derived by subtracting the ACC on congruent flanker trial types from ACC on incongruent trial types. The interference effect for RT was calculated by subtracting incongruent from

congruent RT. These outcomes index the ability of participants to maintain task performance between the two trial types.

ERP assessment

EEG activity was recorded simultaneously during the flanker task via a Neuro-scan Quik-cap with 64 passive, wet, sintered Ag/AgCl scalp electrodes arranged in the international 10–10 system with electrodes placed near the outside each eye and above and below the left eye [29]. A midline sensor placed between CZ and CPZ served as a reference, and AFZ served as the ground. Continuous EEG data was digitized using a Neuroscan SynampsRT amplifier at a sampling rate of 500 Hz, amplified 500 times to an online low-pass 70-Hz filter with a direct current and a 60-Hz notch filter. Electrode impedance values were maintained at ≤20 kohms.

Signal processing and analyses were performed in MATLAB (MathWorks, Natick, MA, version 2021b) using the EEGLab and ERPlab toolbox plug-ins [30,31]. Continuous data were re-referenced to the average of two mastoid electrodes. A trained research team member visually inspected all channels for excessive noise during pre-processing. Channels with excessive noise were interpolated with an average of the adjacent electrodes. Data were submitted to a 0.1 Hz high-pass Butterworth filter before eye-blink artifacts were rejected using independent component analysis (ICA). ICA and vertical eye sensor channel correlations greater than 0.35 were considered eye-blinks. A time window of −200 to 1200 ms around stimulus presentation was used for creating stimulus-locked epochs with a baseline correction of −200 ms to stimulus onset. A 30-Hz low-pass filter was used. Artifacts were detected and rejected if a moving window peak-to-peak amplitude exceeded 100 μV, using a 100 ms window width and step. Only correct trials from individuals who reported >80% of artifact-free trials in all Flanker task trials

186 were included in analyses (>20% artifacts: N=3 CON, N=4 SCF), consistent with previous
187 literature [32,33].
188 Electrodes of interest were chosen based on a collapsed localizer technique[34]. Evidence
189 for selection was observed from maximal voltage localization of combined baseline and post-
190 testing trials collapsed across condition and trial type. Post-hoc topographic average plots were
191 constructed using a stylized topographic map plugin for EEGLAB/ERPLAB[35]. From these plots,
192 the P3 component was defined as a region of interest comprised of C1, CZ, C2, CPZ, CP1, and
193 CP2 with localized peak and corresponding latency between 300 and 600 ms post-stimulus onset.
194
195 *Relational memory assessment*
196 A computerized spatial reconstruction task, iPosition, was used to assess hippocampal-
197 dependent relational memory using Presentation Software (Neurobehavioral Systems, Berkeley,
198 CA) as previously described [36]. Participants viewed six abstract shapes on the computer screen in
199 a randomized array for 6 seconds, which were then masked by small black squares for 18
200 seconds and could be viewed individually by clicking on each square. The boxes then
201 disappeared, and the stimuli reappeared at the top of the screen after a 2-second lag. Participants
202 were asked to reconstruct the randomized array they previously studied for a total of 20 trials.
203 Two error metrics were used to assess performance: misplacement (original misplacement),
204 calculated as the average measure of distance between the actual and reconstructed stimuli
205 locations, and object-location binding (accurate single item placement), the number of times the
206 participant correctly placed a stimulus within a pre-defined radius.
207
208 *Neuropsychological assessment*

The Cambridge Neuropsychological Test Automated Battery (CANTAB, Cambridge Cognition Ltd) was used to test cognitive performance across multiple domains presented on a tablet with a touchscreen. The battery included the Intra-Extra Dimensional Set Shift (IED), Stop Signal Task (SST), Rapid Visual Information Processing (RVP), and Spatial Working Memory (SWM). The IED is a test of executive function and assesses rule acquisition and reversal, attentional set formation, maintenance, and shifting. The RVP task assesses sustained attention, The SST measures response inhibition. The SWM task assesses spatial working memory.

Mood States and Psychological assessment

Mood and psychological functioning were assessed using four validated self-report instruments: the Profile of Mood States (POMS), the Positive and Negative Affect Schedule (PANAS), and the Perceived Stress Scale (PSS). The POMS is a 65-item questionnaire that evaluates transient mood states across six subscales (Tension-Anxiety, Depression-Dejection, Anger-Hostility, Vigor-Activity, Fatigue-Inertia, and Confusion-Bewilderment), with participants rating how they felt "right now" on a 5-point Likert scale ranging from 0 ("not at all") to 4 ("extremely")[37]. The PANAS consists of 20 items, evenly divided into positive and negative affect subscales, where participants indicate to what extent they generally experience each emotion using a 5-point scale from 1 ("very slightly or not at all") to 5 ("extremely")[38]. The PSS includes 10 items designed to assess perceived stress over the past month, with responses on a 5-point scale ranging from 0 ("never") to 4 ("very often") [39]. Physical activity was assessed using the Godin-Shephard Leisure-Time Exercise Questionnaire, measuring the frequency of strenuous, moderate, and light physical activities performed for more than 15 minutes during a

231 typical week. A total leisure activity score was calculated using the weighted formula: (9 x
232 strenuous) + (5 x moderate) + (3 x light).
233
234 *Fecal collection and processing*
235 During the five days before starting each intervention condition and the last five days
236 during their last week (days 25-30) of each treatment and washout period, participants were
237 asked to provide two fecal samples for each timepoint (2 x PRE and 2 x POST for both SCF and
238 CON). Participants were instructed to provide fecal samples within 15 minutes of defecation
239 using provided materials, including Commode Specimen Collection Systems (Sage Products),
240 ice packs, and coolers. Samples were homogenized upon arrival in the laboratory, aliquoted into
241 cryovials for sequencing, flash-frozen in liquid nitrogen, and stored at -80°C. Fecal samples were
242 also aliquoted into 15mL test tubes for phenol/indole measurements, pre-weighed aluminum tins
243 to calculate the dry matter basis (DMB), and acidified with 2N-HCl (10% wt:vol) for SCFAs
244 (acetate, propionate, butyrate), BFCAs (valerate, isovalerate, isobutyrate), and ammonia; these
245 aliquots were all frozen at -20°C until analysis. A fecal pH measurement (Denver Instrument)
246 was also recorded for each sample.
247
248 *Fecal DNA isolation and 16S amplicon analyses*
249 Fecal microbial DNA was extracted utilizing the Power-Lyzer PowerSoil DNA Isolation
250 Kit (QIAGEN). DNA quality was assessed using 1% agarose gel, and concentrations were
251 measured using a Qbit 3.0 Fluorometer (ThermoFisher Scientific). Extracted DNA from the two
252 fecal samples collected at each time point were pooled in equimolar amounts and sequenced at
253 the University of Illinois W. M Keck Center for Biotechnology. 16S amplicon sequencing

254 utilized V4 primers (forward (F): 5'-GTGYCAGMGCCGCGGTAA, reverse (R): 5'-
255 GGACTACNVGGGTWTCTAAT) with a NovaSeq 6000 SP with 2x250nt to produced ~1
256 billion reads. High-quality (quality score > 25) sequence data were filtered using DADA2[40]
257 integrated within QIIME2 software (v2023.7)[41]. Sequences were denoised and resolved into
258 amplicon sequence variants (ASVs) using the SILVA 138-99 (515F/806R) naïve Bayes
259 reference classifier [40,42]. After quality filtering, samples were rarefied to a depth of 350,000
260 sequences, corresponding to the minimum sampling depth across all samples. At this sequencing
261 depth, rarefaction curves plateaued across all samples, indicating sufficient coverage of amplicon
262 ASVs (**Supplemental Figure 2**). Rarefaction was performed using the vegan package (v2.6.8)[43]
263 with a fixed pseudo-random number generator (set.seed = 8) in RStudio (v2024.12.0). No library
264 was driven to zero counts. Rarefaction removed 1,521 of the original 11,894 ASVs (13%): 909
265 were singletons, and 612 had zero counts in the unrarefied dataset. A total of 10,373 ASVs
266 (87%) were retained for analyses.
267 Alpha and beta diversity measures were performed with the R vegan and phyloseq
268 (v1.48.0)[44] package. Alpha diversity was calculated using phyloseq for richness and Shannon
269 indices. Then, a linear mixed effect model with treatment-by-time interaction and the participant
270 was utilized as the random intercept. Bray-Curtis dissimilarities (distance(method="bray")) and
271 weighted UniFrac distances (distance(method="wunifrac")) were also calculated using phyloseq.
272 We then performed PERMANOVA via adonis2() (vegan) with 5,000 permutations to assess the
273 effects of treatment, time, and their interaction on community composition, and tested for
274 homogeneity of group dispersions with betadisper() and permutest(). For visualization the
275 function ordinate(method="PCoA") and plot_ordination()

276 Differential abundance was conducted on normalized rarefied feature table using
277 phylotype_analysis. Relative abundance was used for visualization and table summaries (sweep,
278 MARGIN=1, rowSums). Before modeling differential abundance, the count data were filtered to
279 improve model stability and reduce noise. First, genera with a total count of zero across all
280 samples were removed. Next, a minimum total read count threshold was applied, retaining only
281 genera with at least 0.01% reads across all samples. A prevalence filter was also used, retaining
282 taxa present (nonzero counts) in at least 40% of samples. The generalized linear mixed effect
283 modeling included only taxa meeting the filtering criteria.
284 Predictive metagenomics analyses were conducted using PICRUSt2 (v2.5.3)[45] to assess
285 the functional potential for each sample from the complete cohort (picrust2_pipeline.py with
286 default parameters)[45,46]. The output includes the ko mapping (ko_info), unstratified KO, and EC-
287 predicted metagenome files, which were used for broad function and pathway differential
288 abundance analyses with the R-package ggpicrust2 (v.1.7.3)[47] using LinDA method. The KO-
289 predicted metagenome (KO pred metagenome contrib) file was used for a granular analysis for
290 all KOs using the R-package MaAsLin2 (v1.18.0)[47,48]. The parameters set in MaAsLin2 included
291 a fixed effect of the treatment, a random effect of participant, a 50% minimum prevalence
292 (default 10%), and the default *P*-adjustment (FDR). This was between the baseline, end-to-end,
293 and baseline compared to the respective end-point. We selected carbohydrate metabolism-related
294 pathways and KEGG orthologs to limit the KOs investigated. The mapping files were imported
295 using R-package KEGGREST (v112.1) to create a filtering vector which included:
296 Glycolysis/Gluconeogenesis (map00010), Pentose phosphate pathway (map00030), Fructose and
297 mannose metabolism (map00500), Pyruvate metabolism (map00620), Butanoate metabolism
298 (map00650), and additional KOs including alpha-amylase (K01176), alpha-amylase glycosidase

299 (K01223), beta-glucosidase (K01210), Glucan 1,4-alpha-glucosidase (K01190), alpha-
300 glucosidase (K01187), alpha glucosidase GH183 and GH97 (K012348). The predicted KO
301 metagenome stratified file provided the normalized taxon contribution
302 (norm_taxon_function_contrib) for each KO, allowing the genera-level visualization of
303 contribution for the selected associated KOs to compare between treatments.
304
305 *Microbial Metabolites*
306 Fecal dry matter was measured according to the methods of the Association of Official
307 Analytical Chemists, 1984[49]. Ammonia concentrations were determined using methods outlined
308 by Chaney and Marbach[50]. Fecal sample aliquots for SCFA and BCFA concentrations were
309 weighed, acidified with 2N hydrochloric acid, and stored at -20°C until analysis. Before analysis,
310 samples were thawed at room temperature for 15 minutes and centrifuged at 13,000*g* for 10 min.
311 Gas chromatography mass spectroscopy (GC-MS) was used for quantification, normalized by
312 dry matter weight[51]. Phenol and indole concentrations were quantified, according to Flickiet al.
313 et al.[52]. Fecal metabolite concentrations are reported on a dry matter basis.
314
315 *Digestive health*
316 Gastrointestinal symptoms, bowel function, and stool characteristics were measured
317 using 7-day self-reported records, questionnaires, and stool processing in the laboratory before
318 and after each intervention period[53]. The 7-day self-reported gastrointestinal symptom records
319 included subjective ratings (1 [absent], 2 [mild], 3 [moderate], and 4 [severe]) for burping,
320 cramping/pain, distension/bloating, flatulence/gas, nausea, reflux (heartburn), and rumblings.
321 Participants also recorded their bowel movement consistency (1 [separate hard lumps], 2

322 [sausage-shaped but lumpy], 3 [sausage-like but with cracks on the surface], 4 [sausage-like,
323 smooth, and soft], 5 [soft blobs with clear cut edges], 6 [fluffy pieces, mushy], and 7 [entirely
324 liquid]) and ease of passage (1 [very easy], 2 [easy], 3 [neither easy nor difficult], 4 [difficult], 5
325 [very difficult]). In the laboratory, upon collection of each fresh fecal sample, pH was measured
326 using a pH meter (Denver Instrument)[53]. A trained research team member recorded their
327 assessment of the Bristol stool consistency of the fecal sample.
328
329 *In vitro culturing of Parabacteroides distasonis*
330 Utilizing an adapted protocol from Garcia-Bayona et al[54]. *Parabacteroides distasonis*
331 (*Pd*) -- 31_2 (deposited as *Porphyromonas* sp., Strain 31_2, HM-169) was obtained through
332 Biodefense and Emerging Infections Research Resources Repository (BEI Resources), National
333 Institute of Allergy and Infectious Diseases (NIAID), National Institute of Health (NIH) as part
334 of the Human Microbiome Project in anaerobic brain heart infusion (BHI) and chopped meat
335 media. To test the effects of different carbohydrate sources, an M9 minimal medium was
336 prepared and supplemented with essential nutrients, including 50 mg/L L-cysteine, 5 mg/L
337 hemin, 2.5 µg/L vitamin K1, 2 mg/L FeSO4·7H2O, and 5 µg/L vitamin B12. The carbohydrate
338 sources added to the M9 medium were either 0.25% (wt/vol) glucose (M9-Glu), 0.25% CON
339 (M9-CON), or 0.4% (wt/vol) SCF (M9-SCF). As a positive control, the BHI medium was used
340 to verify the *P. distasonis* strain viability. The M9 medium without any added carbohydrates
341 served as a negative control to confirm that no other medium component contributed to bacterial
342 growth. Additionally, each medium had a blank control containing no *Pd* inoculum to ensure no
343 contamination and allowed any background noise from the media to be subtracted.

344 Hemin stock solution was prepared at a final concentration of 5 mg/L by dissolving 10
345 mg of powdered hemin in 10 mL of 0.05 M NaOH. The solution was sterilized using a 0.22 µm
346 filter and stored at 4°C. Vitamin K1 stock solution was prepared to a final concentration of 2.5
347 µg/L, 2.5 mg of powdered vitamin K1 was dissolved in 0.5 mL of 100% ethanol, followed by
348 dilution to 10 mL with sterile distilled water. The solution was sterilized via filtration and stored
349 at 4°C. L-cysteine hydrochloride solution was prepared to a concentration of 50 mg/L by
350 dissolving 100 mg of L-cysteine in 10 mL of sterile molecular-grade water. The solution was
351 filter sterilized and stored at 4°C. To ensure sterility, all solutions were prepared within a
352 chemical fume hood and biosafety cabinet. *Pd* was cultured overnight in BHI broth. A 20 µL
353 aliquot of the overnight culture was inoculated into 180 µL of M9 medium, achieving a 1:10
354 dilution and a starting OD_{600} at approximately 0.1 absorbance.
355 Three biological replicates consisting of three technical replicates for each per treatment
356 were plated on a 10 x 10 honeycomb plate. The Bioscreen-C was programmed to measure the
357 OD_{600} at regular intervals (30 min), the lowest interval setting allowed using a 600 nm brown
358 filter while maintaining a temperature of 37°C and shaking for 5 seconds before and after each
359 reading. OD_{600} measurements were collected for 25.5 hrs using BioScreen-C for each biological
360 and technical replicate for each substrate and the triple blanks (no *Pd* inoculate) for each
361 technical replicate (**Supplemental Figure 3**). The blank samples would confirm no growth
362 without any inoculation in the media with and without a substrate. Since all cultures reached the
363 stationary phase by 14 hrs across all the carbohydrates, statistical analyses were restricted to the
364 first 14 hrs. Optical density readings were adjusted by subtracting blank values to remove
365 background media noise for downstream analyses.

366 $$\text{Adjusted OD} = \text{OD}_{\text{Sample}} - \text{OD}_{\text{Blank}}$$

367 Growth rates were calculated at 2-hr intervals throughout the first 14 hrs to capture the
368 dynamic changes in bacterial growth across different carbohydrate sources. For each biological
369 replicate, the specific growth rate (μ) was calculated as the slope between consecutive $\ln(OD_{600})$
370 values over 2-hour intervals, where time (hrs) served as the independent variable and $\ln(OD_{600})$
371 as the dependent variable.

372 $$\text{Growth rate } (\mu) = \frac{\ln(\mathrm{OD}_t) - \ln(\mathrm{OD}_{t-2})}{2}$$

373

374 *Genomic analyses of a subsample of responders and non-responders*

375 Shotgun metagenomics utilized a subsample population (N = 6) of responders (n=3) and
376 non-responders (n=3), including PRE and POST fecal samples from the SCF condition.
377 Responder status was determined based on a participant's delta enrichment of *Parabacteroides*
378 following the SCF intervention (**Supplemental Figure 4**). Delta values were calculated using the
379 relative abundance values for each participant. A positive delta value was categorized as
380 responders, while a negative or null delta was categorized as non-responders. The samples
381 selected for metagenomic sequencing were from participants with the three lowest and three
382 highest delta values (responders).

383 The whole metagenome for the 12 fecal DNA samples (baseline and end samples from
384 the SCF condition for three responders and three non-responders) was sequenced at the W. M.
385 Keck Center for Biotechnology at the University of Illinois Urbana-Champaign. Libraries were
386 pooled, quantified by qPCR, and sequenced on one half of a 10B lane for 151 cycles from both
387 ends of the fragments using a NovaSeq X Plus with V1.0 sequencing kits. FastQ files were
388 generated and demultiplexed with the bcl2fastq v2.20 Conversion Software (Illumina). Adapters
389 (CTGTCTCTTATACACATCT) were trimmed from the 3'-end of the reads. The quality scores

390 in the FastQ files used an ASCII offset of 33, known as Sanger scores. Shotgun metagenomic
391 data processing and bioinformatics analyses were performed using the Carl R. Woese Institute
392 for Genomic Biology (IGB) Biocluster at the University of Illinois at Urbana-Champaign.
393 Pre-processing was performed using KneadData (v0.12.0) for quality control and host
394 contaminant removal on paired-end FASTQ files, utilizing 25 processing threads for optimized
395 parallel processing. Trimmomatic (v0.39) was employed for adapter removal and quality
396 trimming, while Tandem Repeat Finder (TRF) was used to identify and remove repetitive
397 sequences. Quality control reports were generated at multiple stages using FastQC (v0.11.9).
398 Host DNA sequences were filtered against the KneadData database (20230405 release). The
399 cleaned, high-quality paired-end reads were concatenated per sample using the --cat-final-output
400 flag for downstream processing. Taxonomic profiling was conducted using MetaPhlAn[55]
401 (v4.0.6), which employed Bowtie2 (v2.5.0) to align reads against the ChocoPhlAnSGB_202212
402 reference database. The kneaddata-filtered FASTQ files were analyzed using the
403 rel_ab_w_read_stats mode, normalizing taxonomic abundances while preserving read count
404 information using 25 processing threads. Following taxonomic profiling, individual sample
405 profiles were merged to generate study-wide abundance tables. The merge_metaphlan_tables.py
406 script [55] aggregates relative abundance profiles across all samples. To develop an absolute
407 abundance table, we used a modified script (merge_metaphlan_tables_abs.py), which included a
408 single-line modification to allow the merging of absolute abundances instead of relative values.
409 The script was obtained from BioBakery (https://github.com/timyerg/Metaphlan-absolute-
410 abundance-merger/) and requires that MetaPhlAn be run with -t rel_ab_w_read_stats to capture
411 read count information alongside relative abundances as described earlier. Functional profiling of
412 microbial communities was conducted using HUMAnN (v3.7)[56] to characterize gene families

413 and metabolic pathways. HUMAnN3 was applied to the kneaddata-filtered FASTQ files,
414 utilizing taxonomic profiles generated by MetaPhlAn to improve species-resolved functional
415 annotation. The analysis incorporated the ChocoPhlAn nucleotide database (v201901b) and the
416 UniRef90 protein database (November 2024) to stratify gene functions at the species level.
417 Following functional profiling, UniRef90 gene family identifiers were mapped to their respective
418 protein descriptions using the HUMAnN "human_rename_table" function for interpretable
419 annotations for downstream analyses.

420 For gene family analyses, we conducted log fold comparisons between responders and
421 non-responders $\log_2$[(delta R/delta NR)]. All gene families with a log fold change >2 were
422 selected, yielding over 2000 gene family clusters. To focus on carbohydrate-active gene families,
423 a targeted filtering approach was applied using key terms associated with carbohydrate
424 metabolism, including "Alpha-amylase," "Glycoside hydrolase," "Glycosyl hydrolase,"
425 "acetate," "butyrate," "propionate," "pyruvate," "Glycosyl transferase," "hexokinase,"
426 "glucokinase," "glucose," and "carbohydrate." This refinement reduced the dataset to 217 gene
427 families, from which the top 40 with the highest positive log fold change were selected for a
428 correlation heatmap using z-normalized abundance values.

429 CAZy was utilized to determine higher resolution of carbohydrate-active enzymes[57,58]
430 from the metagenomic data in responders and non-responders. Raw sequencing reads were pre-
431 processed using Trim Galore (v0.6.0) to remove adapter sequences and low-quality bases, and
432 contaminants were identified using Kraken2 (v2.1.1) with a standard database. Clean reads were
433 assembled into contigs using MEGAHIT (v1.2.9); assembly quality was assessed by applying a
434 minimum contig length threshold (≥1000 bp) and examining general assembly statistics provided
435 by MEGAHIT. Gene prediction and annotation were conducted using Prokka (v1.4), generating

436 protein sequences and gene annotations. CAZyme annotation was performed using run_dbcan
437 (v4.0.0)[59], employing three methods: HMMER searched against the dbCAN HMMdb for
438 CAZyme family-level annotation, DIAMOND searched against CAZy annotated protein
439 sequences, and HMMER search against the dbCAN-sub HMMdb for substrate prediction. The
440 outputs included annotated CAZymes, their associated families, predicted CGCs (Carbohydrate-
441 active Gene Clusters), and substrate assignments based on the dbCAN-sub HMMdb and
442 validated PUL (Polysaccharide Utilization Loci) datasets. To quantify CAZyme abundances,
443 clean reads were mapped to coding sequences and contigs using BWA (v0.7.17-r1188), with
444 sorting performed via Samtools (v1.7) and read counts calculated using Bedtools (v2.27.1).
445 Abundance metrics such as transcripts per million were computed using dbcan_utils scripts
446 within the run_dbcan package[59]. The workflow was executed on a Linux computer with 128 GB
447 RAM, utilizing Anaconda (v23.7.3) for environment management to streamline software
448 installation and dependency handling.
449

450 **Statistical analyses**

451 The study's primary outcomes were assessed using a linear mixed effect model for an
452 end-to-end comparison between conditions with baseline values included as a covariate. For
453 example, the Flanker task ACC following each intervention (SCF and CON) was analyzed using
454 linear mixed-effects models, controlling for baseline ACC on the flanker task within each
455 condition. Data was analyzed in R version 4.4.3. using the packages: “lme4” (v1.1.37),
456 “glmmTMB “(v1.1.11), “lmerTest” (v3.1.3), “emmeans” (v1.11.0), “Hmisc” (v5.2.3), “rstatix”
457 (v0.7.20, “coin” (v1.4.3), “vegan” (v2.6.10), “phyloseq” (v1.48.0), “MaAsLin2” (v1.18.0),
458 “ggpicrust2” (v2.0.0), “interactions” (v1.2.0), and “mediation” (v4.5.0) [45,47,48,60–64]. Data and

residuals were examined for normality using the Shapiro-Wilk statistic, visually inspected using Q-Q plots, and homogeneity of variances was tested using Levene's test. Linearity between baseline covariates and response variables was assessed using simple linear models. The α-level was set at 0.05 (two-tailed). For all regression models, the standardized beta coefficients (β_{std}) and 95% CI were calculated using the "parameters" (v0.25.0) package in R.

Log transformation was applied to acetate, propionate, and total SCFA, while a square root transformation was applied to RT Interference, Peak Latency, PANAS, POMS, Godin valerate, isovalerate, total BCFA, and ammonia to meet assumptions for the linear mixed effect model. Two Flanker task ACC scores, two ERP mean amplitudes, and one fecal butyrate concentration were winsorized due to extreme outliers (>3 standard deviations)[65,66]. For congruent models, if an interaction between congruency and treatment with $P<0.05$, then a *post-hoc* was conducted between treatment for each congruency with Benjamini-Hochberg *P*-adjustment (method = "BH").

A linear mixed effect model was applied to microbiota alpha diversity metrics, while beta diversity was assessed using permutational multivariate analysis of variance (PERMANOVA) with 5,000 permutations, both using treatment by time as fixed effects and ID for the random intercept. The 16S microbiota data, as part of the secondary outcomes, were assessed using generalized linear mixed models fitted with a negative binomial distribution and a log link function (family = nbinom2(link = "log")) [67–69]. For each taxon, a null model, which included only a random intercept for participant ID, was compared to a full model that included treatment by time as fixed effects and a random effect for participant ID. Including baseline abundance as a covariate caused model instability or singularity issues; therefore, this analysis did not use the baseline covariate model. Model comparisons were conducted using likelihood ratio tests (LRTs)

482 assessed with anova() to determine whether the addition of fixed effects (treatment, time, and
483 their interaction) significantly improved model fit compared to the null model. False discovery
484 rate (FDR) correction was applied across all genera and phyla using the qvalue() function to
485 adjust for multiple hypothesis testing. Taxa with significant LRT q-values (FDR $P < 0.05$) were
486 subjected to *post-hoc* analysis using the least square means (emmeans) to perform pairwise
487 comparisons between treatments within each time (PRE and POST), *post-hoc P*-values were
488 further adjusted (method = "BH") to control for multiple comparisons.

489 The Wilcoxon signed-rank test was applied to gastrointestinal symptoms and CANTAB
490 data (IBM, Armonk, NY, USA) due to the inability to meet linear model assumptions. Delta
491 scores (POST minus PRE) stratified by treatment (SCF and CON) were analyzed for these
492 outcomes to evaluate intervention effects.

493 Analysis of the in vitro *Pd* growth utilized a linear mixed-effects model to compare
494 growth rates across different carbohydrate sources (SCF, CON, glucose) at each time point, with
495 biological replicate (BioRep) included as a random effect to account for repeated measures. Post-
496 hoc pairwise comparisons were performed using BH adjustment to identify significant
497 differences between growth rates at each interval [70].

498 Mediation analyses consisted of two linear regression steps: (1) a mediator model
499 predicting the mediator from treatment, adjusted for baseline mediator levels, and (2) an outcome
500 model predicting cognitive response (i.e.- congruent RT) from treatment and the mediator,
501 adjusted for baseline response of the cognitive measure and baseline mediator levels.
502 Bootstrapped mediation analyses were performed using the mediate function from the R package
503 "mediation" (v4.5.0), employing 8000 bootstrap simulations to estimate the average causal
504 mediation effect (ACME), direct effect (ADE), total effect, and proportion mediated. Sensitivity

505 analyses were performed using the medsens() function from the mediation package to assess the
506 robustness of the mediation results to potential violations of the sequential ignorability
507 assumption, ensuring the measured effects are not biased by unobserved confounding factors.
508 Moderation analyses were conducted to examine whether fecal microbiota and metabolites
509 moderated the relationship between treatment and cognitive measures (e.g.- congruent RT).
510 Separate moderation models were fitted for each moderator (e.g.- *Parabacteroides*). Each model
511 included the interaction term between treatment (as.factor, reference = CON) and the centered
512 moderator variable (center = TRUE, scale = FALSE), adjusted for baseline of the response
513 measure and baseline levels of each respective moderator. Moderator variables were mean-
514 centered to facilitate interpretation. If an interaction effect was flagged as significant, post-hoc
515 analysis using the Jonhson-Neyman (JN) method with the function sim_slope() from the R
516 package "interaction" (v4.4.3) and least square means were employed, verifying the moderation
517 simple slopes and effects at low (-1 SD), mean, and high (+1 SD) moderator levels.
518

519 **Results**

520 *Participant characteristics*

521 The study consort (**Figure 1**) demonstrates the study recruitment, enrollment, and
522 retention flow. Forty-two participants were randomized, and forty-one completed the study
523 (Table 1). Forty-two participants completed cognitive outcomes, including the 1 participant who
524 dropped after their first period, for 41 CON and 42 SCF. Data from participants who completed
525 and were compliant (consumed >80% of supplement sachets measured by their compliance logs)
526 during at least one of their condition periods (PRE and POST for a treatment) were included in
527 the per-protocol analyses (38 CON and 39 SCF) for primary outcomes. For ERP P3 amplitudes,

528 there were three missing data points for CON (1=PRE, 2=POST) and seven missing for SCF
529 (2=PRE, 5=POST). Two participants could not provide fecal samples during the respective
530 collection periods, therefore, a total of 39 participants (38 CON, 37 SCF) were used for
531 secondary outcomes.
532
533 *Cognitive outcomes*
534 Behavioral Flanker Task performance was assessed using ACC and RT outcomes (**Table**
535 **2**). There were no significant treatment effects for ACC ($P = 0.32$) and no treatment x
536 congruency interaction ($P = 0.40$), with most participants maintaining high levels of task
537 accuracy (≥92%) across all conditions. In contrast, RT outcomes revealed a significant main
538 effect of treatment ($P < 0.001$), with participants responding faster following SCF than CON.
539 Both baseline ($P < 0.001$; $\eta^2 = 0.27$) and RT interference ($P < 0.001$; $\eta^2 = 0.16$) were significant
540 covariates. *Post-hoc* comparisons using estimated marginal means indicated that SCF reduced
541 RTs by 8.26 ms in congruent trials (FDR $P = 0.03$, SE: 3.62, 95% CI: [1.03, 15.5 ms]) and by
542 11.81 ms for incongruent trials (FDR $P = 0.002$, SE: 3.61, 95% CI: [4.60 to 19.0 ms]) compared
543 to CON (**Supplemental Figure 5**). In a separate model with RT interference as the outcome with
544 baseline adjustment, participants who consumed SCF resolved interference more efficiently,
545 demonstrating a 4.33 ms faster resolution than CON ($P < 0.001$, SE: 1.27, 95% CI: [1.82, 6.83
546 ms]). ERP distribution of the P3 amplitude was visualized (**Supplemental Figure 6**), and mean
547 amplitude did not statistically differ between treatment groups ($P = 0.91$). No main congruency
548 effect was detected ($P = 0.67$) or in the treatment-by-congruency interaction ($P = 0.80$).
549 Similarly, the peak latency of the P3 component did not differ by treatment ($P = 0.29$) or the

interaction (P = 0.38); however, there was a congruency effect (P = 0.02). Standardized beta coefficients are presented in Table 2.

There were no statistical differences between PANAS and PSS measures (P > 0.29; **Supplemental Table 1**). The PSS had no statistical difference between conditions (P=0.43). Performance across all CANTAB measures yielded null results (all P > 0.13; **Supplemental Table 2-5**). POMS subscales and TMD, Godin physical activity scores, and the iPosition task had no statistically significant treatment effects (all P > 0.46; **Supplemental Table 6**).

Metabolomics

No statistically significant differences in SCFA or BCFA concentrations were observed (all P > 0.12; **Table 3**). Notably, SCF consumption numerically increased fecal acetate by ~11.3% (P=0.12, estimate: -0.12, SE: 0.08, 95% CI:[-0.28, 0.03]) compared to CON. Phenol, indoles, and ammonia results are presented in **Supplemental Table 7**. Pooled total indole concentrations (including indole, 2-methylindole, 3-methylindole, and 7-methylindole) tended to be lower following SCF consumption (P=0.09, estimate: 0.23, SE: 0.13, 95% CI: [-0.04, 050]). Phenol and ammonia concentrations did not differ between treatments (all P > 0.26). Standardized beta coefficients are presented in Table 3.

Gastrointestinal symptoms

Gastrointestinal symptom severity scores remained within the absent-to-mild range for most participants, with no significant differences observed between treatments for cramping, nausea, reflux, rumbling, or burping (all P > 0.17; **Table 4**). However, gas severity increased with SCF compared to CON (P=0.01), with 33% of SCF participants reporting moderate-to-

severe symptoms at the end-point compared to 16% in the CON group. Bloating severity also increased after SCF (*P*=0.05). Stool characteristics, including self-reported consistency and ease of passage measures, and pH did not differ between the CON and SCF conditions (all $P > 0.12$; **Supplemental Table 8**).

16S Fecal microbiota

A significant treatment-by-time interaction was observed for richness ($P = 0.01$) and *post-hoc,* demonstrating a difference between treatments at end-point (FDR $P < 0.001$, estimate: 29.11, SE: 8.16, 95% CI: [12.9, 45.3]) but not at baseline (FDR *P*=0.95). Shannon diversity had no significant interaction effect (*P*=0.26) (**Supplemental Figure 7**). Standardized beta coefficients are presented in **Table 5**. There was no significant treatment-by-time interaction in Beta diversity measured by weighted UniFrac (R^2= 0.0072, *P*=0.35) or Bray-Curtis (R^2= 0.0055, *P*=0.76; **Supplemental Figure 8).**

A total of 260 genera were initially detected in the dataset. After applying prevalence and abundance filtering criteria, 128 genera were retained, and 14 met the significance threshold of FDR < 0.05 (**Supplemental Figure 9**). Significant genera classified as *incertae sedis* and with extremely low relative abundance at the end-point (11; <0.5%) are presented in **Supplemental Table 9.** *Post-hoc* pairwise comparisons were performed on the log scale estimates from the log-linked negative binomial models. *Parabacteroides* abundance had a significant treatment-by-time interaction (FDR $P < 0.001$; Table 5, **Figure 2);** *post-hoc* pairwise comparison between treatments at end-point demonstrated a 4.14-fold increase enrichment with SCF (FDR $P < 0.001$, estimate: -1.42, SE: 0.16, 95% CI: [-1.74, -1.11]) with no difference detected between baseline (FDR *P*=0.91, estimate: 0.02, SE: 0.16, 95% CI: [-0.29, 0.33]). *Fusicatenibacter* also had a

596 significant interaction effect (FDR $P < 0.001$); *post hoc* comparison between treatments at end-
597 points demonstrated a 2.64-fold increase with SCF (FDR $P<0.001$, estimate: -0.97, SE: 0.18,
598 95% CI: [-1.34, -0.60]), no difference at baseline (FDR $P=0.64$, estimate: 0.14, SE: 0.19, 95%
599 CI: [-0.23, 0.50]). *Dialister* similarly had an interaction effect (FDR $P = 0.02$); *post hoc*
600 demonstrated a 2.43-fold increase at end-point with SCF (FDR $P = 0.003$, estimate: -0.89, SE:
601 0.30, 95% CI: [-1.48, -0.30]), and also no difference at baseline (FDR $P=0.50$, estimate: 0.17,
602 SE: 0.26, 95% CI: [-0.33, 0.68]). Genus-level relative abundances and model FDR adjusted
603 treatment-by-time interaction and standardized beta coefficients are presented in Table 5
604 At the phylum level, 8 of the 15 detected phyla met filtering criteria, but none met the
605 significance threshold, phylum-level results shown in **Supplemental Table 10**.
606
607 *Correlation analyses*
608 As part of the third aim**,** the analyses tested relationships between microbial abundances,
609 SCFAs, and congruent RT in the Flanker task to explore task-related cognitive performance. The
610 Spearman correlation analysis explored relationships between reaction time for each congruency
611 type, SCFA concentrations, and *Parabacteroides* after SCF plotted in a heatmap (**Figure 3).**
612 Congruent RT was inversely associated with acetate ($\rho = -0.328$, $P=0.048$) and propionate
613 concentrations ($\rho = -0.356$, $P=0.031$). Incongruent RT was not significantly correlated with any
614 SCFA (P-values > 0.3). *Parabacteroides* relative abundance exhibited a significant positive
615 correlation with acetate ($\rho = 0.343$, $P=0.038$). However, *Parabacteroides* were not significantly
616 associated with congruent ($\rho = -0.194$, $P=0.25$) or incongruent RT ($P = 0.99$). In contrast,
617 *Fusicatenibacter* and *Dialister* showed numeric positive correlations with congruent RT ($\rho =$
618 0.30, $P=0.08$ and $\rho = 0.31$, $P=0.06$, respectively) demonstrated in **Supplementary Figure 10.**

619

620 *Mediation analyses*

621 This analysis (**Table 6**) evaluated fecal microbiota and metabolites as potential mediators
622 between treatment and congruent RT. Acetate did not significantly mediate the effect of
623 treatment on congruent RT (P=0.22, 95% CI: [-4.32, 0.78]). However, the direct impact of
624 treatment (ADE), representing effects independent of acetate, remained statistically significant
625 (P=0.03, 95% CI: [-22.99, -2.36]). The overall treatment effect (combining direct and mediated
626 pathways) was significant (P=0.01, 95% CI: [-24.27, -3.77]). The proportion mediated by acetate
627 was estimated at 11.4% (P=0.23, 95% CI: [-0.107, 0.54]). Sensitivity analysis for acetate
628 demonstrated that the confounding of both the mediator and outcome relationships would need to
629 explain approximately 4% of the shared variance to nullify the mediation effect.

630 Similarly, propionate, *Parabacteroides*, and *Fusicatenibacter* did not significantly
631 mediate the treatment's effect on congruent RT (all ACMEs $P \geq 0.1$), although the direct and
632 total effects of treatment remained significant in each case (all ADE and total effects $P \leq 0.05$).
633 Sensitivity analysis for propionate, *Fusicatenibacter*, and *Parabacteroides* similarly
634 demonstrated <2% shared variance to nullify the mediation effect.

635

636 *Moderation analyses*

637 For this analysis, we used 16S fecal microbiota (*Parabacteroides*) and fecal SCFA
638 (acetate and propionate) as moderators to evaluate their strength or direction on the relationship
639 between treatment and congruent RT. **Table 7** presents the standardized regression coefficients
640 from the moderation models. The relationship between treatment and congruent RT was
641 influenced by the abundance of *Parabacteroides*, exhibiting a statistically significant moderation

642 effect ($\beta = 0.29$, P=0.03). *Post-hoc* analyses using estimated marginal means and simple slopes
643 (**Figure 4**) also demonstrated a diminishing effect from *Parabacteroides*, significantly
644 moderating the treatment effect at –1 standard deviation ($\beta_{-1} = -24.17$, $P < 0.001$), marginally at
645 the centered mean level ($\beta_0 = -9.95$, P=0.10), but not at the higher end ($\beta_{+1} = 4.27$, P=0.68).
646
647 *In vitro culturing of Pd measuring growth rates*
648 The quick growth confirms the utilization of the simpler carbohydrates, and differing
649 growth rates at later time points for the fermentation of the fiber (**Figure 5a**). Peak OD_{600} was
650 highest in the SCF (0.60 abs at 13 hrs), followed by glucose (0.59 abs at 5.5 hrs) and CON (0.54
651 abs at 5 hrs). Mixed-effects modeling revealed significant main effects of media, time, and their
652 interaction (all FDR $P < 0.001$). *Post-hoc* comparisons confirmed a diauxic growth pattern in
653 SCF-treated cultures, which exhibited lower OD_{600} at 2 and 4 hrs (FDR $P < 0.001$) but higher
654 OD_{600} at 8 and 10 hrs compared to glucose and CON (FDR $P < 0.001$) (**Figure 5b**). No
655 significant differences were detected at 6 hrs and at the last time point (14 hrs). The blank control
656 remained significantly lower than all other treatments across all time points (FDR $P < 0.001$).
657
658 *PICRUSt predicted metagenomic analyses*
659 Unstratified KEGG Orthology (KO) analysis identified N-glycan biosynthesis and alpha-
660 linolenic acid metabolism pathways as significantly different between SCF and CON at end-
661 point (FDR $P < 0.01$; **Supplemental Figure 11a**). The corresponding unstratified EC analysis
662 also detected 23 enzyme functions differential between the treatments (FDR $P < 0.05$;
663 **Supplemental Figure 11b**). Significant pairwise differences were only detected between SCF at
664 end-point relative to all other time points, and no differences were found between CON and

665 baseline periods. From the MaAsLin2 analysis, we detected 2,701 carbohydrate-metabolism KOs
666 significantly associated with SCF at end-point (FDR $P < 0.05$), with the top 20 positive
667 coefficients shown in **Figure 6**. Additional pair-wise comparisons further gave resolution
668 between pairs detecting 1,778 significant KOs between PRE and POST SCF, four between PRE
669 and POST CON, and none between baseline periods. Among the top SCF-associated KOs, 18
670 were contributed by *Parabacteroides* and two by *Fusicatenibacter* (**Supplemental Figure 12**).
671
672 *MetaPhlaN and HUMAnN analyses on Microbial Responder and Non-Responders*
673 Summary analyses of genus-level relative abundances (**Supplemental Table 10,**
674 **Supplemental Figure 13**) suggest observable differences between SCF microbial responders
675 and non-responders. *Parabacteroides* was confirmed more abundant in responders' post-
676 intervention (13.6%) and remained low or undetectable in non-responders. At the species level
677 (**Supplemental Figure 14**), *Pd* and *P. merdae* appeared to increase in responders (10.9% and
678 2.7%, respectively) but were low or undetected in non-responders post-intervention (<0.5%).
679 Using HUMAnN, delta abundance analyses were conducted to examine microbial
680 contributions to carbohydrate metabolism-related KOs in responders and non-responders (**Figure**
681 **7**). Responders showed post-treatment increases in several gene families, including UDP-glucose
682 6-dehydrogenase, alpha-amylase, and hexokinase. In non-responders, KO abundances remained
683 relatively stable between PRE and POST time points. Genus- and species-level comparisons
684 (**Supplemental Figure 15** and **Figure 8,** respectively) demonstrate increased post-treatment
685 contributions from *Pd* across multiple carbohydrate-active genes, including glycoside hydrolases
686 (GHs), alpha-amylase, and hexokinase.
687

688 *CAZy analyses of GH in microbial Responders and Non-responders*

689 When available and provided by CAZy databases, GH family and subfamilies were used
690 to compare log fold changes between responders and non-responders. From the 228 identified
691 GH families, we isolated those with positive log fold abundances in responders (**Supplemental**
692 **Figure 16**). Among the identified GH families, GH43_8, GH43_33, GH25, GH24, GH179,
693 GH13_9, GH130_2, and GH123 were abundantly present in responders and positively correlated
694 with *Parabacteroides* abundance (**Supplemental Figure 17**).

695

696 **Discussion**

697 In this randomized crossover trial, SCF consumption improved attentional inhibition,
698 demonstrated by faster RTs without sacrificing ACC measured by the modified flanker task. No
699 significant effects were observed for relational memory, perceived stress, mood, affect, or
700 neuropsychological function (as assessed by the iPosition task, PSS, POMS, PANAS, and
701 CANTAB, respectively). Microbiota analyses revealed an increase in *Parabacteroides* after
702 consuming SCF. There was a numeric increase in fecal acetate and mild gastrointestinal
703 intolerance symptoms. Functional analyses (predictive and shotgun metagenomics) suggested
704 enhanced carbohydrate metabolism, with *Pd* emerging as the primary SCF-responsive species. *In*
705 *vitro* culturing confirmed *Pd's* ability to metabolize SCF directly.

706 Few clinical trials have assessed the impact of dietary fiber on cognitive performance
707 while integrating microbiome analyses. Herein, SCF consumption selectively enhanced
708 attentional inhibition, a core executive function component, without impacting memory, mood,
709 or sacrificing accuracy. This suggests that SCF may support more efficient cognitive control,
710 particularly in resolving conflicting information and maintaining task-relevant focus. Our results
711 support emerging evidence that fibers may influence brain function via the gut-brain axis. Prior

712 studies have observed that other fibers, such as inulin, improve mood[26], but cognitive benefits
713 appear domain-specific and may depend on the fiber type, population, and study duration.
714 Consistent with previous SCF trials, *Parabacteroides* was enriched following the
715 intervention[16,71,72], and we identified *Pd* as the primary species. Notably, an inverse relationship
716 was observed between *Pd* and *Bacteroides vulgatus,* suggesting dynamic microbial competition
717 or adaption to SCF availability.
718 Functional predictions and metagenomic data revealed increased carbohydrate
719 metabolism and glycan degradation pathways following SCF consumption[73]. CAZy-based
720 functional annotation revealed GH enrichment within *Pd*, including GH13 and GH144, key
721 enzymes for metabolizing complex carbohydrates. *Parabacteroides* have been shown to harbor
722 carbohydrate-active enzymes, including GHs such as GH144, GH35, GH13, GH43 and
723 GH73[73,74]. GH144 and GH13, found specifically in *P*d, contribute to β-1,2-
724 glucooligosaccharides hydrolysis, while GH13 is involved in the hydrolysis of α-1,6 glycosidic
725 bonds, allowing it to break down both complex and simple carbohydrate structures like SCF to
726 hold its place within the large intestine ecology[74].
727 Our *in vitro* experiment confirmed that *Pd* directly fermented SCF, with a diauxic
728 pattern, likely due to the mixture of SCF and non-fiber carbohydrates within the sachets. This
729 functional evidence, together with *in vivo* enrichment and metagenomic data, strongly supports
730 *Pd's* direct role in SCF fermentation.
731 Although fecal acetate only increased numerically with SCF consumption, SCFAs remain
732 strong candidates as mediators of gut-brain signaling. Indeed, SCFAs can positively affect
733 cognitive and affective processes through microbiota-dependent and independent
734 mechanisms[21,23]. For example, increasing colonic propionate through inulin-propionate ester

735 consumption influenced anticipatory brain reward response in healthy men[21], while
736 administering an SCFA mixture to the colon of healthy men for one-week reduced cortisol
737 response to an acute psychosocial stress challenge[21]. SCFAs in systemic circulation can cross the
738 blood-brain barrier (BBB) and directly impact brain health[23,75,76]. However, in our study,
739 mediation analyses did not support a direct causal role for SCFA or individual taxa in cognitive
740 performance. Moderation analyses indicated that the relationship between SCF consumption and
741 cognitive performance was moderated by *Parabacteroides* abundance. Interestingly, the
742 moderating influence diminished at higher abundance thresholds, where greater *Parabacteroides*
743 abundance was associated with slower RTs. These findings suggest threshold effects,
744 emphasizing the complexity of host-microbiome interactions.

745 In summary, our results demonstrated that SCF is selectively utilized by
746 *Parabacteroides*, which underpins cognitive benefits. A prebiotic is defined as "a substrate that
747 is selectively utilized by host microorganisms, conferring a health benefit"[75]. Within this
748 framework, our findings demonstrate SCF's prebiotic capability for modulating the gut
749 microbiota with meaningful implications for cognitive performance in healthy older adults.
750 Notably, *Parabacteroides* emerged as a consistent keystone taxon, enriched in 90% of
751 participants following SCF consumption, consistent with the Health-Associated Core Keystone
752 (HACK) index[76], which identified *Pd* as a core and stability-associated taxon[78]. Indeed, *Pd* has
753 been associated with health, including anti-inflammatory effects and gut barrier protection[77–79]
754 and bioactive metabolite production (i.e., gamma-aminobutyric acid (GABA)[80]), implicated in
755 gut-brain communication, which highlights *Pd's* potential as a next-generation probiotic
756 candidate[73,77–79,81,82].

757 Given that our sample was predominantly white, female, and highly educated, the
758 generalizability of these results is a limitation of the present work. Also, although metagenomic
759 sequencing was conducted to identify species and characterize shifts in microbiome functional
760 capacity following SCF consumption, these analyses were limited to a subsample of responders
761 and non-responders. Additionally, we did not collect blood, precluding assessment of systematic
762 SCFA or other circulating biomarkers. Finally, the fecal metabolite panel was limited in scope
763 and may have missed relevant compounds involved in gut-brain communication. Despite these
764 limitations, this study contributes novel evidence linking a specific fermentable fiber to selective
765 cognitive benefits, with mechanistic insights into microbiota responses and SCFA profiles.
766 Future studies should employ broader multi-omics analyses, dose-response designs, and systemic
767 biomarkers assessment to better elucidate the mechanisms underlying microbiota-mediated
768 cognitive outcomes and advance precision nutrition strategies.
769

770 **Acknowledgments**

771 We thank Dr. Michael J. Miller and Dr. Pratik Banerjee, and their graduate students, for
772 providing the *Pd* strain, facility, and equipment to perform the *in vitro* growth culturing
773 component of this research. We would like to thank the graduate and undergraduate research
774 assistants from the Holscher and Khan laboratories for their assistance during the clinical
775 appointments and data entry.
776

777 **Author Disclosures**

778 The authors report no conflict of interest.
779

780 **Author contributions**

781 The authors' responsibilities were as follows – HDH, NAK, DAA, TAH: designed the
782 research; MDB, TM: recruited and enrolled participants and coordinated study procedures;
783 DAA: conducted the *in vitro* experiment; DAA, TAH, SM, TM, RS: conducted the experiments
784 and testing appointments; MA, DR, DAA: managed biological samples collection and storages;
785 DAA, TAH: managed study data; DAA, NS: prepared data for bioinformatic pipelines; DAA,
786 TAH: analyzed the data: DAA, TAH, NAK, HDH: wrote the manuscript; NAK, HDH: had
787 primary responsibility for final content; and all authors: read and approved the final manuscript.
788
789

References

1. Morris MC, Wang Y, Barnes LL, Bennett DA, Dawson-Hughes B, Booth SL. Nutrients and bioactives in green leafy vegetables and cognitive decline: Prospective study. *Neurology*. 2018;90(3):E214-E222. doi:10.1212/WNL.0000000000004815
2. Perim Baldo M, Aboussaleh Y, Turrini A, et al. Adherence to a Mediterranean-Style Diet and effects on Cognition in Adults: A Qualitative evaluation and Systematic Review of Longitudinal and Prospective Trials. 2016;3:1. doi:10.3389/fnut.2016.00022
3. Khan NA, Raine LB, Donovan SM, Hillman CH. IV. The cognitive implications of obesity and nutrition in childhood. *Monogr Soc Res Child Dev*. 2014;79(4):51-71. doi:10.1111/mono.12130
4. Fleming SA, Monaikul S, Patsavas AJ, Waworuntu R V., Berg BM, Dilger RN. Dietary polydextrose and galactooligosaccharide increase exploratory behavior, improve recognition memory, and alter neurochemistry in the young pig. *Nutr Neurosci*. 2019;22(7):499-512. doi:10.1080/1028415X.2017.1415280
5. Gronier B, Savignac HM, Miceli M Di, et al. Increased cortical neuronal responses to NMDA and improved attentional set-shifting performance in rats following prebiotic (B-GOS s) ingestion. doi:10.1016/j.euroneuro.2017.11.001
6. Khan NA, Raine LB, Drollette ES, Scudder MR, Kramer AF, Hillman CH. Dietary Fiber Is Positively Associated with Cognitive Control among Prepubertal Children. *J Nutr*. 2015;145(1):143-149. doi:10.3945/JN.114.198457
7. Hassevoort KM, Lin AS, Khan NA, Hillman CH, Cohen NJ. Added sugar and dietary fiber consumption are associated with creativity in preadolescent children. *Nutr Neurosci*. 2020;23(10):791-802. doi:10.1080/1028415X.2018.1558003
8. Naveed S, Venäläinen T, Eloranta AM, et al. Associations of dietary carbohydrate and fatty acid intakes with cognition among children. *Public Health Nutr*. 2020;23(9):1657-1663. doi:10.1017/S1368980019003860
9. Shuan W, Tan K, Fen P, et al. The Role of Soluble Corn Fiber on Glycemic and Insulin Response. doi:10.3390/nu12040961
10. Jakeman SA, Henry CN, Martin BR, et al. Soluble corn fiber increases bone calcium retention in postmenopausal women in a dose-dependent manner: A randomized crossover trial. *American Journal of Clinical Nutrition*. 2016;104(3):837-843. doi:10.3945/ajcn.116.132761
11. Klosterbuer AS, Hullar MAJ, Li F, et al. Gastrointestinal effects of resistant starch, soluble maize fibre and pullulan in healthy adults. doi:10.1017/S0007114513000019
12. Stewart ML, Nikhanj SD, Timm DA, Thomas W, Slavin JL. Evaluation of the effect of four fibers on laxation, gastrointestinal tolerance and serum markers in healthy humans. *Ann Nutr Metab*. 2010;56(2):91-98. doi:10.1159/000275962
13. LinAmy AHM, Nichols BL, Quezada-Calvillo R, et al. Unexpected high digestion rate of cooked starch by the Ct-maltase-glucoamylase small intestine mucosal α-glucosidase subunit. *PLoS One*. 2012;7(5). doi:10.1371/journal.pone.0035473
14. Vester Boler BM, Rossoni Serao MC, Bauer LL, et al. Digestive physiological outcomes related to polydextrose and soluble maize fibre consumption by healthy adult men. *British Journal of Nutrition*. 2011;106(12):1864-1871. doi:10.1017/S0007114511002388
15. Maathuis A, Venema K, Hoffman A, Evans A, Sanders L. The effect of the undigested fraction of maize products on the activity and composition of the microbiota determined in

a dynamic in vitro model of the human proximal large intestine. *J Am Coll Nutr*. 2009;28(6):657-666. doi:10.1080/07315724.2009.10719798

16. Whisner CM, Martin BR, Nakatsu CH, et al. Soluble corn fiber increases calcium absorption associated with shifts in the gut microbiome: A randomized dose-response trial in free-living pubertal females. *Journal of Nutrition*. 2016;146(7):1298-1306. doi:10.3945/jn.115.227256
17. Arroyo MC, Laurie I, Rotsaert C, Marzorati M, Risso D, Karnik K. Age-Dependent Prebiotic Effects of Soluble Corn Fiber in M-SHIME® Gut Microbial Ecosystems. *Plant Foods for Human Nutrition*. 2023;78(1):213-220. doi:10.1007/s11130-023-01043-z
18. Diamond A. Executive functions. *Annu Rev Psychol*. 2013;64:135-168. doi:10.1146/annurev-psych-113011-143750
19. Duncan-Johnson CC. P300 latency: A new metric of information processing. *Psychophysiology*. 1981;18(3):207-215. doi:10.1111/j.1469-8986.1981.tb03020.x
20. Polich J. Updating P300: An integrative theory of P3a and P3b. *Clinical Neurophysiology*. 2007;118(10):2128-2148. doi:10.1016/j.clinph.2007.04.019
21. La Torre D, Verbeke K, Dalile B. Dietary fibre and the gut–brain axis: microbiota-dependent and independent mechanisms of action. *Gut Microbiome*. 2021;2. doi:10.1017/gmb.2021.3
22. Dalile B, Fuchs A, La Torre D, Vervliet B, Van Oudenhove L, Verbeke K. Colonic butyrate administration modulates fear memory but not the acute stress response in men: A randomized, triple-blind, placebo-controlled trial. *Prog Neuropsychopharmacol Biol Psychiatry*. 2024;131. doi:10.1016/j.pnpbp.2024.110939
23. Cheng J, Hu H, Ju Y, et al. Gut microbiota-derived short-chain fatty acids and depression: deep insight into biological mechanisms and potential applications. *Gen Psychiatr*. 2024;37(1). doi:10.1136/gpsych-2023-101374
24. Luqman A, He M, Hassan A, et al. Mood and microbes: a comprehensive review of intestinal microbiota's impact on depression. *Front Psychiatry*. 2024;15. doi:10.3389/fpsyt.2024.1295766
25. Haskell CF, Scholey AB, Jackson PA, et al. Cognitive and mood effects in healthy children during 12 weeks' supplementation with multi-vitamin/minerals. *British Journal of Nutrition*. 2008;100(5):1086-1096. doi:10.1017/S0007114508959213
26. Leyrolle Q, Cserjesi R, D.G.H. Mulders M, et al. Prebiotic effect on mood in obese patients is determined by the initial gut microbiota composition: A randomized, controlled trial. *Brain Behav Immun*. 2021;94:289-298. doi:10.1016/j.bbi.2021.01.014
27. Erdfelder E, FAul F, Buchner A, Lang AG. Statistical power analyses using G*Power 3.1: Tests for correlation and regression analyses. *Behav Res Methods*. 2009;41(4):1149-1160. doi:10.3758/BRM.41.4.1149
28. Edwards CG, Walk AM, Cannavale CN, et al. Dietary choline is related to neural efficiency during a selective attention task among middle-aged adults with overweight and obesity. *https://doi.org/101080/1028415X20191623456*. 2019;24(4):269-278. doi:10.1080/1028415X.2019.1623456
29. Chatrian GE, Lettich E, Nelson PL. American Journal of EEG Technology Ten Percent Electrode System for Topographic Studies of Spontaneous and Evoked EEG Activities Ten Percent Electrode System for Topographic Studies of Spontaneous and Evoked EEG Activities. Published online 2015. doi:10.1080/00029238.1985.11080163

30. Delorme A, Makeig S. EEGLAB: An open source toolbox for analysis of single-trial EEG dynamics including independent component analysis. *J Neurosci Methods*. 2004;134(1):9-21. doi:10.1016/J.JNEUMETH.2003.10.009
31. Lopez-Calderon J, Luck SJ. ERPLAB: An open-source toolbox for the analysis of event-related potentials. *Front Hum Neurosci*. 2014;8(1 APR):213. doi:10.3389/FNHUM.2014.00213/BIBTEX
32. Kamijo K, Pontifex MB, Khan NA, et al. The association of childhood obesity to neuroelectric indices of inhibition. *Psychophysiology*. 2012;49(10):1361-1371. doi:10.1111/J.1469-8986.2012.01459.X
33. Walk AM, Edwards CG, Baumgartner NW, et al. The role of retinal carotenoids and age on neuroelectric indices of attentional control among early to middle-aged adults. *Front Aging Neurosci*. 2017;9(JUN):183. doi:10.3389/FNAGI.2017.00183/BIBTEX
34. Luck SJ, Gaspelin N. How to get statistically significant effects in any ERP experiment (and why you shouldn't). *Psychophysiology*. 2017;54(1):146-157. doi:10.1111/PSYP.12639
35. Pontifex MB. Stylized Topographic Map Plugin for EEGLAB/ERPLAB.
36. Horecka KM, Dulas MR, Schwarb H, Lucas HD, Duff M, Cohen NJ. Reconstructing relational information. *Hippocampus*. 2018;28(2):164-177. doi:10.1002/hipo.22819
37. Stephen J. Gibson. The Measurement of Mood States in Older Adults. *The Journals of Gerontology: Series B*. 1997;52B(4):167-174.
38. Humboldt S von, Monteiro A, Leal I. Validation of the PANAS: A Measure of Positive and Negative Affect for Use with Cross-National Older Adults. *Rev Eur Stud*. 2017;9(2):10. doi:10.5539/res.v9n2p10
39. Lee EH. Review of the psychometric evidence of the perceived stress scale. *Asian Nurs Res (Korean Soc Nurs Sci)*. 2012;6(4):121-127. doi:10.1016/j.anr.2012.08.004
40. Callahan BJ, McMurdie PJ, Rosen MJ, Han AW, Johnson AJA, Holmes SP. DADA2: High-resolution sample inference from Illumina amplicon data. *Nat Methods*. 2016;13(7):581-583. doi:10.1038/nmeth.3869
41. Bolyen E, Rideout JR, Dillon MR, et al. Reproducible, interactive, scalable and extensible microbiome data science using QIIME 2. *Nat Biotechnol*. 2019;37(8):852-857. doi:10.1038/s41587-019-0209-9
42. Yilmaz P, Parfrey LW, Yarza P, et al. The SILVA and "all-species Living Tree Project (LTP)" taxonomic frameworks. *Nucleic Acids Res*. 2014;42(D1). doi:10.1093/nar/gkt1209
43. Morton JT, Marotz C, Washburne A, et al. Establishing microbial composition measurement standards with reference frames. *Nat Commun*. 2019;10(1). doi:10.1038/s41467-019-10656-5
44. McMurdie PJ, Holmes S. Phyloseq: An R Package for Reproducible Interactive Analysis and Graphics of Microbiome Census Data. *PLoS One*. 2013;8(4). doi:10.1371/journal.pone.0061217
45. Douglas GM, Maffei VJ, Zaneveld JR, et al. PICRUSt2 for prediction of metagenome functions. *Nat Biotechnol*. 2020;38(6):685-688. doi:10.1038/s41587-020-0548-6
46. Langille MGI, Zaneveld J, Caporaso JG, et al. Predictive functional profiling of microbial communities using 16S rRNA marker gene sequences. *Nat Biotechnol*. 2013;31(9):814-821. doi:10.1038/nbt.2676

47. Yang C, Mai J, Cao X, Burberry A, Cominelli F, Zhang L. ggpicrust2: an R package for PICRUSt2 pre-dicted functional profile analysis and visualiza-tion. *Bioinformatics, YYYY*.:0-0. doi:10.1093/bioinformatics/xxxxx
48. Mallick H, Rahnavard A, McIver LJ, et al. Multivariable association discovery in population-scale meta-omics studies. *PLoS Comput Biol*. 2021;17(11). doi:10.1371/journal.pcbi.1009442
49. Kenneth Helrich. *Official Methods for Analysis of the Association of Official Analytical Chemists*.; 1990.
50. Chaney AL, MEP. Modified Reagents for Determination of Urea and Ammonia. *Clin Chem*. 1962;8(2):130-132.
51. Holscher HD, Doligale JL, Bauer LL, et al. Gastrointestinal tolerance and utilization of agave inulin by healthy adults. *Food Funct*. 2014;5(6):1142-1149. doi:10.1039/c3fo60666j
52. Flickinger EA, Schreijen EMWC, Patil AR, et al. Nutrient digestibilities, microbial populations, and protein catabolites as affected by fructan supplementation of dog diets Get access Arrow. *J Anim Sci*. 2003;81(8):2008-2018.
53. Holscher HD, Chumpitazi BP, Dahl WJ, et al. Perspective: Assessing Tolerance to Nondigestible Carbohydrate Consumption. *Advances in Nutrition*. 2022;13(6):2084-2097. doi:10.1093/advances/nmac091
54. García-Bayona L, Comstock LE. Streamlined genetic manipulation of diverse bacteroides and parabacteroides isolates from the human gut microbiota. *mBio*. 2019;10(4). doi:10.1128/mBio.01762-19
55. Blanco-Míguez A, Beghini F, Cumbo F, et al. Extending and improving metagenomic taxonomic profiling with uncharacterized species using MetaPhlAn 4. *Nat Biotechnol*. 2023;41(11):1633-1644. doi:10.1038/s41587-023-01688-w
56. Beghini F, McIver LJ, Blanco-Míguez A, et al. Integrating taxonomic, functional, and strain-level profiling of diverse microbial communities with biobakery 3. *Elife*. 2021;10. doi:10.7554/eLife.65088
57. Drula E, Garron ML, Dogan S, Lombard V, Henrissat B, Terrapon N. The carbohydrate-active enzyme database: Functions and literature. *Nucleic Acids Res*. 2022;50(D1):D571-D577. doi:10.1093/nar/gkab1045
58. Cantarel BI, Coutinho PM, Rancurel C, Bernard T, Lombard V, Henrissat B. The Carbohydrate-Active EnZymes database (CAZy): An expert resource for glycogenomics. *Nucleic Acids Res*. 2009;37(SUPPL. 1). doi:10.1093/nar/gkn663
59. Zheng J, Ge Q, Yan Y, Zhang X, Huang L, Yin Y. DbCAN3: Automated carbohydrate-Active enzyme and substrate annotation. *Nucleic Acids Res*. 2023;51(W1):W115-W121. doi:10.1093/nar/gkad328
60. Kuznetsova A, Brockhoff PB, Christensen RHB. lmerTest Package: Tests in Linear Mixed Effects Models. *J Stat Softw*. 2017;82(13):1-26. doi:10.18637/JSS.V082.I13
61. R Core Team. R: A language and environment for statistical computing. Published online 2013.
62. Czech L, Barbera P, Stamatakis A. Genesis and Gappa: Processing, analyzing and visualizing phylogenetic (placement) data. *Bioinformatics*. 2020;36(10):3263-3265. doi:10.1093/bioinformatics/btaa070
63. Louca S, Doebeli M. Efficient comparative phylogenetics on large trees. *Bioinformatics*. 2018;34(6):1053-1055. doi:10.1093/bioinformatics/btx701

971 64. Ye Y, Doak TG. A parsimony approach to biological pathway reconstruction/inference for
972 genomes and metagenomes. *PLoS Comput Biol*. 2009;5(8).
973 doi:10.1371/journal.pcbi.1000465
974 65. Kwak SK, Kim JH. Statistical data preparation: Management of missing values and
975 outliers. *Korean J Anesthesiol*. 2017;70(4):407-411. doi:10.4097/kjae.2017.70.4.407
976 66. Kafadar K. John Tukey and Robustness. *Statistical Science*. 2003;3(18(3)):319-331.
977 doi:1076102419
978 67. Zhang X, Mallick H, Tang Z, et al. Negative binomial mixed models for analyzing
979 microbiome count data. *BMC Bioinformatics*. 2017;18(1). doi:10.1186/s12859-016-1441-
980 7
981 68. Sweeny AR, Lemon H, Ibrahim A, et al. A mixed-model approach for estimating drivers
982 of microbiota community composition and differential taxonomic abundance. *mSystems*.
983 Published online July 25, 2023. doi:10.1128/msystems.00040-23
984 69. Jamieson PE, Smart EB, Bouranis JA, et al. Gut enterotype-dependent modulation of gut
985 microbiota and their metabolism in response to xanthohumol supplementation in healthy
986 adults. *Gut Microbes*. 2024;16(1). doi:10.1080/19490976.2024.2315633
987 70. Zwietering MH, Jongenburger I, Rombouts FM, Van ' K, Riet T. *Modeling of the*
988 *Bacterial Growth Curve PUm*.; 1990. https://journals.asm.org/journal/aem
989 71. Timm DA, Thomas W, Boileau TW, Williamson-Hughes PS, Slavin JL. Polydextrose and
990 soluble corn fiber increase five-day fecal wet weight in healthy men and women. *Journal*
991 *of Nutrition*. 2013;143(4):473-478. doi:10.3945/jn.112.170118
992 72. Hooda S, Vester Boler BM, Rossoni Serao MC, et al. 454 pyrosequencing reveals a shift
993 in fecal microbiota of healthy adult men consuming polydextrose or soluble corn fiber.
994 *Journal of Nutrition*. 2012;142(7):1259-1265. doi:10.3945/jn.112.158766
995 73. Shimizu H, Nakajima M, Miyanaga A, et al. Characterization and Structural Analysis of a
996 Novel exo-Type Enzyme Acting on β-1,2-Glucooligosaccharides from Parabacteroides
997 distasonis. *Biochemistry*. 2018;57(26):3849-3860. doi:10.1021/acs.biochem.8b00385
998 74. Ducarmon QR, Karcher N, Tytgat HLP, et al. Large-scale computational analyses of gut
999 microbial CAZyme repertoires enabled by Cayman. Published online January 8, 2024.
1000 doi:10.1101/2024.01.08.574624
1001 75. Gibson GR, Hutkins R, Sanders ME, et al. Expert consensus document: The International
1002 Scientific Association for Probiotics and Prebiotics (ISAPP) consensus statement on the
1003 definition and scope of prebiotics. *Nat Rev Gastroenterol Hepatol*. 2017;14(8):491-502.
1004 doi:10.1038/nrgastro.2017.75
1005 76. Goel A, Shete O, Goswami S, et al. Toward a health-associated core keystone index for
1006 the human gut microbiome. *Cell Rep*. 2025;44(3):115378.
1007 doi:10.1016/j.celrep.2025.115378
1008 77. Cui Y, Zhang L, Wang X, et al. Roles of intestinal Parabacteroides in human health and
1009 diseases. *FEMS Microbiol Lett*. 2022;369(1). doi:10.1093/femsle/fnac072
1010 78. Cuffaro B, Boutillier D, Desramaut J, et al. Characterization of Two Parabacteroides
1011 distasonis Candidate Strains as New Live Biotherapeutics against Obesity. *Cells*.
1012 2023;12(9). doi:10.3390/cells12091260
1013 79. Ezeji JC, Sarikonda DK, Hopperton A, et al. Parabacteroides distasonis: intriguing
1014 aerotolerant gut anaerobe with emerging antimicrobial resistance and pathogenic and
1015 probiotic roles in human health. *Gut Microbes*. 2021;13(1).
1016 doi:10.1080/19490976.2021.1922241

1017 80. Liang Z, Di N, Li L, Yang D. Gut microbiota alterations reveal potential gut–brain axis
1018 changes in polycystic ovary syndrome. *J Endocrinol Invest*. 2021;44(8):1727-1737.
1019 doi:10.1007/s40618-020-01481-5
1020 81. Wei W, Wong CC, Jia Z, et al. Parabacteroides distasonis uses dietary inulin to suppress
1021 NASH via its metabolite pentadecanoic acid. *Nat Microbiol*. 2023;8(8):1534-1548.
1022 doi:10.1038/s41564-023-01418-7
1023 82. Liu D, Zhang S, Li S, et al. Indoleacrylic acid produced by Parabacteroides distasonis
1024 alleviates type 2 diabetes via activation of AhR to repair intestinal barrier. *BMC Biol*.
1025 2023;21(1). doi:10.1186/s12915-023-01578-2

1026

1027

1028

1029

1030

1031

1032

1033

1034

1035

1036

1037 **Tables**

1038 **Table 1. Baseline Demographic and Clinical Characteristics of Participants Randomized to**

1039 **Maltodextrin or Soluble Corn Fiber Treatments**

	Overall N = 42	**Maltodextrin** N = 21	**Soluble Corn Fiber** N = 21
Education			
High School Graduate	2 (4.8%)	0 (0%)	2 (9.5%)
Some College	6 (14%)	3 (14%)	3 (14%)
Bachelor's Degree	13 (31%)	8 (38%)	5 (24%)
Advanced Degree	21 (50%)	10 (48%)	11 (52%)
Ethnicity			
Asian	6 (14%)	3 (14%)	3 (14%)
Black or African American	3 (7.1%)	1 (4.8%)	2 (9.5%)
Mixed or Other	1 (2.4%)	0 (0%)	1 (4.8%)
White (Caucasian)	32 (76%)	17 (81%)	15 (71%)
Latino	1 (2.4%)	1 (4.8%)	0 (0%)
Sex			
Female	28 (67%)	15 (71%)	13 (62%)
Male	14 (33%)	6 (29%)	8 (38%)
Age (years)	56.2 ± 7.3	54.8 ± 6.2	57.5 ± 8.2
Fiber per 1000kcal	11.4 ± 3.4	12.0 ± 3.3	10.8 ± 3.5
BMI (kg/m²)	25.9 ± 4.0	25.4 ± 3.7	26.3 ± 4.2
Income			
Less than $10,000	1 (2.4%)	0 (0%)	1 (4.8%)
$11,000-20,000	0 (0%)	0 (0%)	0 (0%)
$21,000-30,000	0 (0%)	0 (0%)	0 (0%)
$31,000-40,000	3 (7.1%)	1 (4.8%)	2 (9.5%)
$41,000-50,000	3 (7.1%)	1 (4.8%)	2 (9.5%)
$51,000-60,000	3 (7.1%)	2 (9.5%)	1 (4.8%)
$61,000-70,000	4 (9.5%)	1 (4.8%)	3 (14%)
$71,000-80,000	5 (12%)	4 (19%)	1 (4.8%)
$81,000-90,000	1 (2.4%)	1 (4.8%)	0 (0%)
$91,000-100,000	7 (16.7%)	4 (19%)	3 (14%)
Greater than $100,000	15 (35.7%)	7 (33%)	8 (38%)

1040 Baseline characteristics of participants enrolled and randomized into the clinical trial (N = 42),
1041 stratified by initial treatment assignment. Continuous variables are reported as mean ± standard
1042 deviation; categorical variables are reported as number of participants and percentage within
1043 each group [n (%)].

1044 **Table 2. Behavioral and ERP Outcomes During the Flanker Task Across Timepoints and**

1045 **Treatment Conditions**

	Maltodextrin		**Soluble Corn Fiber**		
	PRE	**POST**	**PRE**	**POST**	
Behavioral Flanker	Mean ± SEM *(n)*	Mean ± SEM *(n)*	Mean ± SEM *(n)*	Mean ± SEM *(n)*	*Treatment*
Accuracy					*P:* 0.32
Congruent	96.87 ± 0.52 *(39)*	95.50 ± 1.37 *(39)*	97.04 ± 0.48 *(40)*	97.64 ± 0.45 *(40)*	95% CI: [-0.10, 0.49]
Incongruent	92.37 ± 1.00 *(39)*	92.04 ± 1.53 *(39)*	93.60 ± 0.79 *(40)*	94.35 ± 0.70 *(40)*	β: 0.20
Reaction Time					***P:* <0.001*** **
Congruent	395.13 ± 5.79 *(39)*	**398.44 ± 6.69**[a] *(39)*	400.71 ± 6.22 *(40)*	**389.49 ± 5.52**[b] *(40)*	95% CI: [-0.34, -0.02]
Incongruent	430.89 ± 6.62 *(39)*	**437.29 ± 7.77**[a] *(39)*	435.43 ± 6.88 *(40)*	**423.99 ± 6.35**[b] *(40)*	β: -0.18
ERP Flanker					
Amplitude					*P:* 0.96
Congruent	5.96 ± 1.73 *(39)*	6.78 ± 0.68 *(36)*	6.64 ± 0.60 *(39)*	7.07 ± 0.77 *(37)*	95% CI: [-0.31, 0.21]
Incongruent	6.36 ± 1.64 *(39)*	6.77 ± 0.69 *(36)*	7.14 ± 0.65 *(39)*	7.50 ± 0.79 *(37)*	β: -0.05
Peak Latency					*P:* 0.28
Congruent	385.68 ± 6.71 *(39)*	399.11 ± 10.18 *(36)*	394.49 ± 7.29 *(39)*	398.06 ± 7.99 *(37)*	95% CI: [-0.12, 0.17]
Incongruent	424.43 ± 8.34 *(39)*	442.88 ± 11.70 *(36)*	438.54 ± 9.90 *(39)*	428.76 ± 8.27 *(37)*	β: 0.02

1046 Mean ± standard error of the mean (SEM) and n values for behavioral and electrophysiological

1047 measures recorded during the Flanker task under congruent and incongruent conditions, stratified

1048 by treatment and timepoint. Measures include accuracy (%), reaction time (ms), P3 amplitude

1049 (μV), and P3 peak latency (ms). Linear mixed effect models included participant as a random

1050 effect, treatment-by-congruency interaction, and baseline covariate for the respective outcome;

1051 ACC and RT models included the flanker effect (Incongruent-Congruent). *Post-hoc* pairwise

comparisons conducted within each congruency condition if Treatment $P < 0.05$. In the table, a, b indicates significant differences within congruency conditions between treatments at end-point after adjusting for baseline. *P* significance threshold used were as follows: '***' <0.001, '**' <0.01, '*' <0.05, '†' <0.1. Standardization was performed by refitting models with z-scored predictors (method = "refit") using parameters (v0.25) package.

1060 **Table 3. Fecal Volatile Fatty Acid Concentrations by Treatment and Timepoint**

	Maltodextrin		Soluble Corn Fiber				
	PRE	**POST**	**PRE**	**POST**			
Short Chain Fatty Acids	Mean ± SEM *(n)*	Mean ± SEM *(n)*	Mean ± SEM *(n)*	Mean ± SEM *(n)*	*P*	β_{Std}	*95% CI*
Butyrate	43.28 ± 4.56 *(38)*	43.90 ± 5.26 *(37)*	38.77 ± 4.58 *(37)*	40.09 ± 3.18 *(37)*	0.83	0.07	[-0.30, 0.45]
Acetate	175.71 ± 13.85 *(38)*	181.71 ± 13.50 *(37)*	165.31 ± 13.24 *(37)*	202.17 ± 14.94 *(37)*	0.12	0.09	[-0.03, 0.22]
Propionate	48.11 ± 3.98 *(38)*	50.80 ± 4.40 *(37)*	47.48 ± 4.32 *(37)*	55.58 ± 4.72 *(37)*	0.19	0.09	[-0.05, 0.23]
Total SCFAs	267.10 ± 21.46 *(38)*	273.04 ± 21.97 *(37)*	255.38 ± 20.58 *(37)*	297.84 ± 22.30 *(37)*	0.13	0.09	[-0.03, 0.23]
Branched Chain Fatty Acids							
Valerate	6.44 ± 0.59 *(38)*	5.99 ± 0.47 *(37)*	6.00 ± 0.47 *(37)*	5.68 ± 0.48 *(37)*	0.58	-0.05	[-0.22, 0.11]
Isobutyrate	6.62 ± 0.54 *(38)*	5.97 ± 0.39 *(36)*	6.29 ± 0.52 *(37)*	5.22 ± 0.33 *(37)*	0.16	-0.26	[-0.61, 0.10]
Isovalerate	9.49 ± 0.82 *(38)*	8.30 ± 0.57 *(36)*	8.66 ± 0.69 *(37)*	7.35 ± 0.54 *(37)*	0.42	-0.14	[-0.48, 0.20]
Total BCFAs	22.55 ± 1.83 *(38)*	20.37 ± 1.31 *(37)*	20.96 ± 1.56 *(37)*	18.25 ± 1.14 *(37)*	0.64	-0.03	[-0.15, 0.10]

1061 Fecal volatile fatty acids measured pre- and post-intervention for each condition arm. Values
1062 represent mean ± standard error of the mean (SEM), with sample sizes in parentheses. *P*-values,
1063 standardized beta coefficients (β_{Std}), and 95% confidence intervals (CI) are derived from linear
1064 mixed effects models with a random intercept for participant ID and fixed effects for treatment
1065 and baseline (PRE) values. Standardization was performed by refitting models with z-scored
1066 predictors (method = "refit") using parameters (v0.25) package.

1067

1068 **Table 4. Self-Reported Gastrointestinal Symptoms by Treatment and Timepoint**

	Maltodextrin		**Soluble Corn Fiber**		
	PRE	**POST**	**PRE**	**POST**	
GI Symptoms	Median [IQR] *(n)*	Median [IQR] *(n)*	Median [IQR] *(n)*	Median [IQR] *(n)*	*P*
Gas	1.57 [0.84] *(39)*	**1.43 [1.00]** *(39)*	1.57 [0.97] *(38)*	**1.93 [1.00]** *(38)*	**0.01***
Cramping	1.00 [0.00] *(39)*	1.00 [0.00] *(39)*	1.00 [0.00] *(38)*	1.00 [0.14] *(38)*	0.91
Bloating	1.00 [0.14] *(39)*	1.00 [0.14] *(39)*	1.00 [0.14] *(38)*	1.00 [0.32] *(38)*	0.05†
Nausea	1.00 [0.00] *(39)*	1.00 [0.00] *(39)*	1.00 [0.00] *(38)*	1.00 [0.00] *(38)*	0.17
Reflux	1.00 [0.00] *(39)*	1.00 [0.00] *(39)*	1.00 [0.03] *(38)*	1.00 [0.00] *(38)*	0.84
Rumbling	1.00 [0.16] *(39)*	1.00 [0.16] *(39)*	1.00 [0.17] *(38)*	1.00 [0.41] *(38)*	0.68
Burping	1.00 [0.16] *(39)*	1.00 [0.00] *(39)*	1.00 [0.28] *(38)*	1.00 [0.17] *(38)*	0.70

1069 Median and interquartile range (IQR) scores for gastrointestinal symptoms reported at baseline
1070 (PRE) and post-intervention (POST) for each condition. Symptom severity was rated on a 4-
1071 point scale (1 = Absent, 2 = Mild, 3 = Moderate, 4 = Severe). Between-treatment comparisons of
1072 change scores were assessed using paired Wilcoxon signed-rank tests. Reported values include
1073 *P*-values. †$P < 0.1$, *$P < 0.05$.

1074

1075

1076

1077

1078

1079

1080 **Table 5. 16S Alpha Diversity and Differential Abundance of Genera from Human Fecal**

1081 **Samples by Treatment and Timepoint**

	Maltodextrin		**Soluble Corn Fiber**				
	PRE	**POST**	**PRE**	**POST**			
Genus (% of sequence)	Mean ± SEM *(n)*	Mean ± SEM *(n)*	Mean ± SEM *(n)*	Mean ± SEM *(n)*	FDR *P*	β_{Std}	*95% CI*
Bacteroides	25.23 ± 1.77 *(38)*	23.70 ± 1.90 *(38)*	27.32 ± 2.06 *(37)*	22.60 ± 2.07 *(37)*	0.11	-0.15	[-0.34, 0.05]
Faecalibacterium	10.19 ± 1.02 *(38)*	10.12 ± 1.11 *(38)*	8.66 ± 1.15 *(37)*	11.02 ± 1.30 *(37)*	0.47	0.23	[-0.18, 0.64]
Parabacteroides	2.52 ± 0.35[a] *(38)*	**2.06 ± 0.24[a]** *(38)*	2.09 ± 0.26[a] *(37)*	**8.37 ± 0.98[b]** *(37)*	**<0.001*** **	1.44	[1.01, 1.88]
Alistipes	3.46 ± 0.51 *(38)*	2.82 ± 0.35 *(38)*	3.88 ± 0.59 *(37)*	3.96 ± 0.69 *(37)*	0.50	0.08	[-0.31, 0.46]
Blautia	3.76 ± 0.50 *(38)*	4.52 ± 0.61 *(38)*	3.54 ± 0.42 *(37)*	3.24 ± 0.50 *(37)*	0.10†	-0.27	[-0.52,-0.02]
Agathobacter	4.16 ± 0.88 *(38)*	5.97 ± 1.17 *(38)*	3.99 ± 0.85 *(37)*	2.80 ± 0.58 *(37)*	0.11	-0.46	[-0.91, 0.01]
Subdoligranulum	2.31 ± 0.29 *(38)*	2.54 ± 0.38 *(38)*	3.24 ± 0.58 *(37)*	2.69 ± 0.49 *(37)*	0.83	-0.24	[-0.68, 0.19]
Prevotella	0.87 ± 0.41 *(38)*	1.64 ± 0.74 *(38)*	1.60 ± 0.89 *(37)*	2.13 ± 1.04 *(37)*	0.53	-0.22	[-0.81, 0.37]
Dialister	1.34 ± 0.44[a] *(38)*	**1.46 ± 0.51[a]** *(38)*	0.93 ± 0.34[a] *(37)*	**2.10 ± 0.63[b]** *(37)*	**0.02***	1.06	[0.29, 1.83]
Bifidobacterium	2.50 ± 0.53 *(38)*	2.69 ± 0.53 *(38)*	2.12 ± 0.52 *(37)*	2.09 ± 0.41 *(37)*	0.92	0.09	[-0.51, 0.70]
Fusicatenibacter	0.60 ± 0.10[a] *(38)*	**0.67 ± 0.09[a]** *(38)*	0.53 ± 0.11[a] *(37)*	**1.79 ± 0.28[b]** *(37)*	**<0.001*** **	1.10	[0.59, 1.61]
Alpha diversity metrics					*P*	β_{Std}	*95% CI*
Richness	439.92 ± 19.80[a] *(38)*	**438.68 ± 18.21[a]** *(38)*	443.57 ± 17.57[a] *(37)*	**413.73 ± 18.56[b]** *(37)*	**0.01***	-0.25	[-0.45,-0.05]
Shannon	3.89 ± 0.06 *(38)*	3.88 ± 0.06 *(38)*	3.81 ± 0.06 *(37)*	3.71 ± 0.07 *(37)*	0.26	-0.20	[-0.56, 0.15]

1082 Values represent mean ± standard error of the mean (SEM), with sample sizes in parentheses.

1083 For 16S data, FDR-adjusted *P*-values reflect the treatment-by-time interaction from generalized

1084 linear mixed effect models with a negative binomial distribution and log-link. For alpha

1085 diversity, *P*-values represent treatment-by-time interactions from linear mixed effect model. All
1086 models included a random intercept for participant ID. Standardized beta coefficients (β_{Std}), and
1087 95% confidence intervals (CI) was performed by refitting models with z-scored predictors
1088 (method = "refit") using parameters (v0.25) package. *Post-hoc* pairwise analysis was conducted
1089 on genera meeting the FDR $P < 0.05$ (16S) or $P < 0.05$ (alpha diversity) for the interaction term.
1090 Superscript letters (a, b) indicate significant pairwise differences between treatments within
1091 timepoints after BH adjustment. Significance *P* thresholds: †$P < 0.1$, *$P < 0.05$, ***$P < 0.001$.
1092
1093

1094 **Table 6. Mediation Effects of 16S Fecal Microbiota and Metabolites on the Relationship**

1095 **Between SCF and Congruent Reaction Time at end-point**

1096

Mediator	Flanker Task	Effect	Estimate	[95% CI]	*P*
Parabacteroides	Congruent RT	Mediation effect	0.24	[-5.32, 4.85]	0.91
		Direct effect	-14.26	[-24.55, -2.89]	0.02
		Total effect	-14.02	[-24.20, -3.61]	0.01
		Proportion Mediated	-1.7%	[-0.57, 0.53]	0.91
Fusicatenibacter	Congruent RT	Mediation effect	0.86	[0.79, 3.40]	0.30
		Direct effect	-14.65	[-25.75, -4.12]	0.01
		Total effect	-13.79	[-23.91, -3.76]	0.01
		Proportion Mediated	-6.2%	[-0.28, 0.08]	0.30
Acetate	Congruent RT	Mediation effect	-1.42	[-4.32, 0.78]	0.22
		Direct effect	-10.98	[-22.99, -2.36]	0.03
		Total effect	-12.39	[-24.27, -3.77]	0.01
		Proportion Mediated	11.4%	[-0.11, 0.54]	0.23
Propionate	Congruent RT	Mediation effect	-1.06	[-3.59, 0.96]	0.33
		Direct effect	-12.82	[-23.65, -2.58]	0.01
		Total effect	-13.88	[-24.2, -3.61]	0.01
		Proportion Mediated	7.6%	[-0.09, 0.38]	0.33

1097 Mediation analysis, frequentist approach, was performed using nonparametric bootstrapped

1098 linear regression models with the mediation (v4.5.0) package to estimate the indirect

1099 (mediation), direct, and total effects of treatment on congruent reaction time (RT), with fecal

1100 *Parabacteroides*, *Fusicatenibacter*, acetate, and propionate as mediators (n = 37). Proportion

1101 mediated reflects the percent of the total effect explained by the indirect pathway.

1102

1103

1104 **Table 7. Moderation Effects of Fecal Microbiota and Metabolites on the Association**

1105 **Between SCF and Congruent Reaction Time at end-point**

Moderator	Flanker Task	Effect	Estimate	SE	[95% CI]	*P*
Parabacteroides	Congruent RT	Main effect	-0.35	3.78	[-7.91, 7.21]	0.08
		Moderation effect	0.29	3.26	[-6.22, 6.79]	**0.03***
Fusicatenibacter	Congruent RT	Main effect	-0.09	3.2	[-6.49, 6.31]	0.57
		Moderation effect	0.03	3.10	[-6.16, 6.23]	0.79
Acetate	Congruent RT	Main effect	-0.19	9.05	[-18.26, 17.89]	0.07
		Moderation effect	0.08	11.68	[-23.25, 23.41]	0.43
Propionate	Congruent RT	Main effect	-0.17	7.38	[-14.90, 14.56]	0.11
		Moderation effect	0.09	10.23	[-20.35, 20.52]	0.34

1106 Moderation analysis was conducted using linear regression models including interaction terms

1107 between treatment and each moderator (n = 37). Models examined whether selected genera (CLR

1108 transformed) and metabolites modified the effect of treatment on congruent reaction time (RT).

1109 Reported values include standardized estimates (β), standard errors (SE), 95% confidence

1110 intervals (CI), and *P*-values.

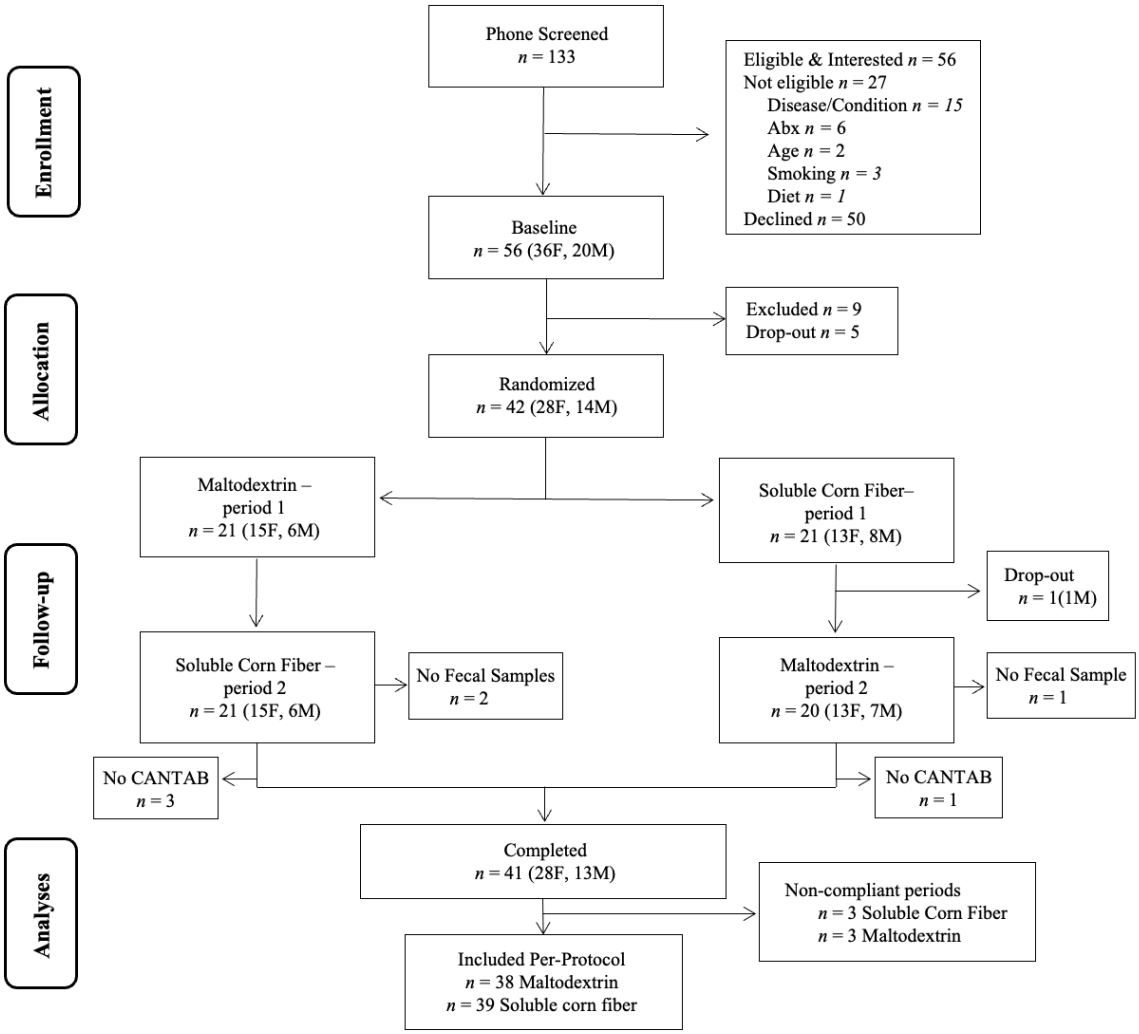

Figure 1. CONSORT (Consolidated Standards of Reporting Trials) Flow Diagram of Participant Recruitment, Randomization, and Retention in the Crossover Trial. Each "*n*" reflects the number of participants at each stage of enrollment, randomization, and follow-up. Following eligibility screening, participants were randomized to begin with either the maltodextrin or soluble corn fiber condition in a counterbalanced crossover design. Participants were retained in the study as long as they completed the primary outcome assessments, including cognitive testing at each intervention timepoint.

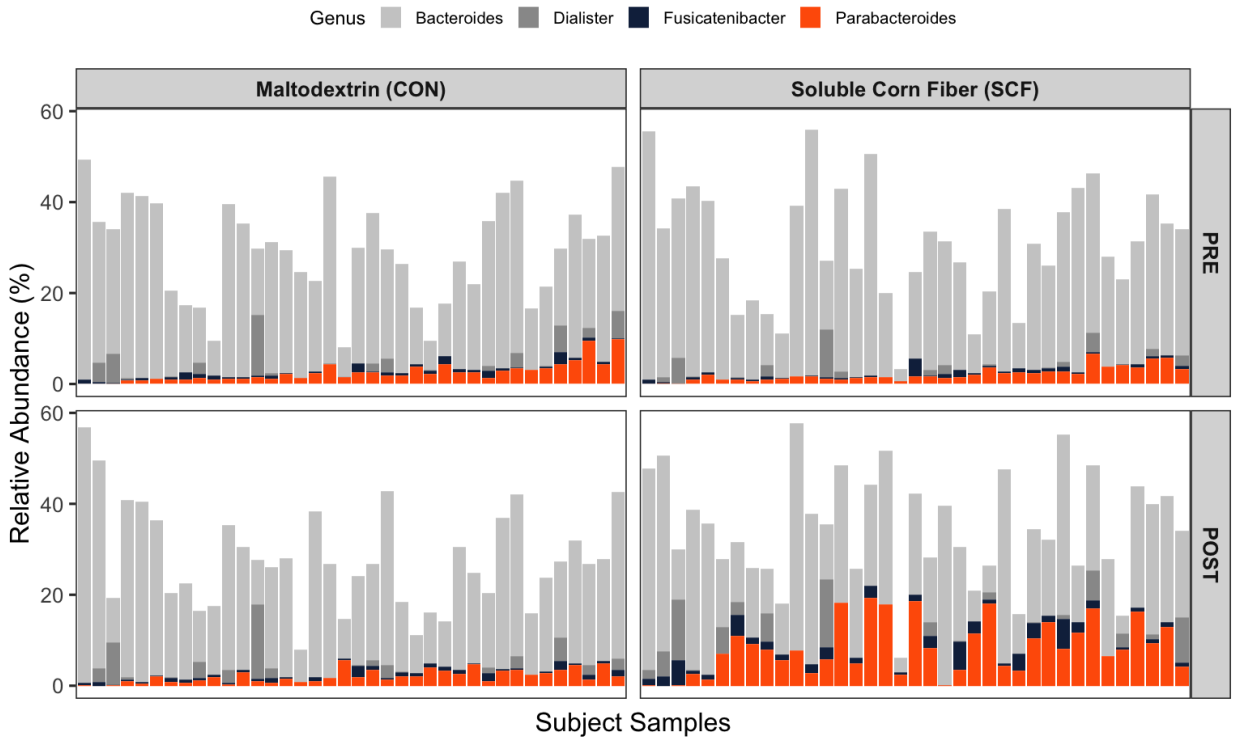

Figure 2. The 16S relative abundance of genera for each subject across both timepoints and treatments. Stacked bar plots display the genus-level composition of the fecal microbiota for each participant across both treatment periods. Relative abundance (%) is expressed as the proportion of total sequences per sample from 16S sequences. Key genera are color-coded: *Parabacteroides* (orange), *Fusicatenibacter* (blue), *Dialister* (dark gray), and *Bacteroides* (gray). Each bar represents a single participant sample at a given timepoint.

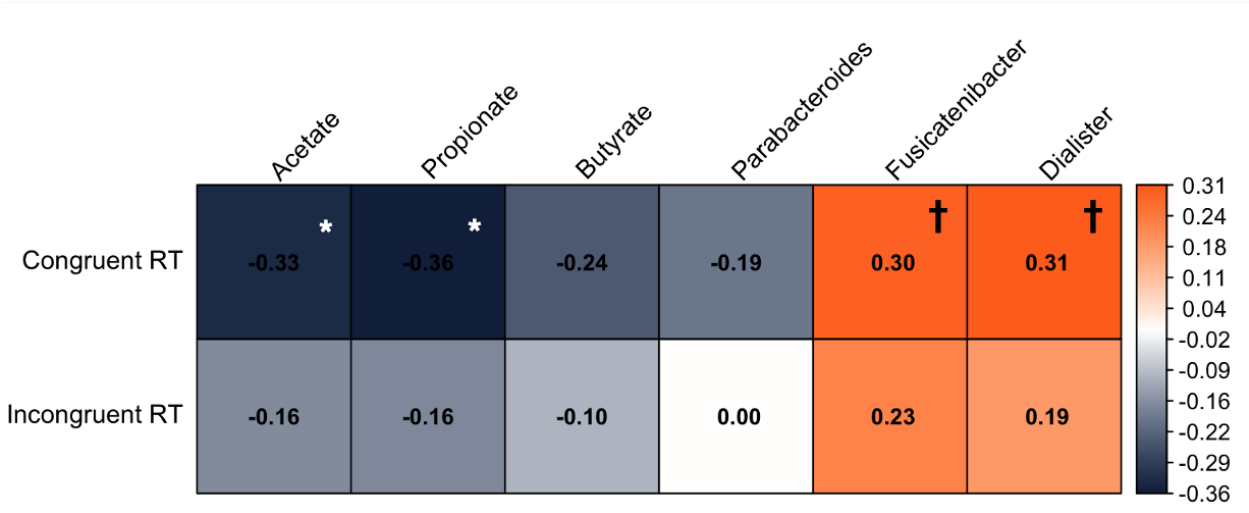

Figure 3. Spearman Correlation Heatmap between Reaction Times and relevant variables following Soluble Corn Fiber Intervention. Heatmap illustrating Spearman correlation coefficients (ρ) among the relative abundance of selected genera identified in 16S differential abundance analysis, fecal SCFA concentrations, and reaction times from both Flanker trials (n = 37; SCF arm only). Positive correlations are shown in orange, negative correlations in blue, with shading intensity reflecting the magnitude of the correlation. Statistical significance is annotated as follows: *P < 0.05; †P < 0.1.

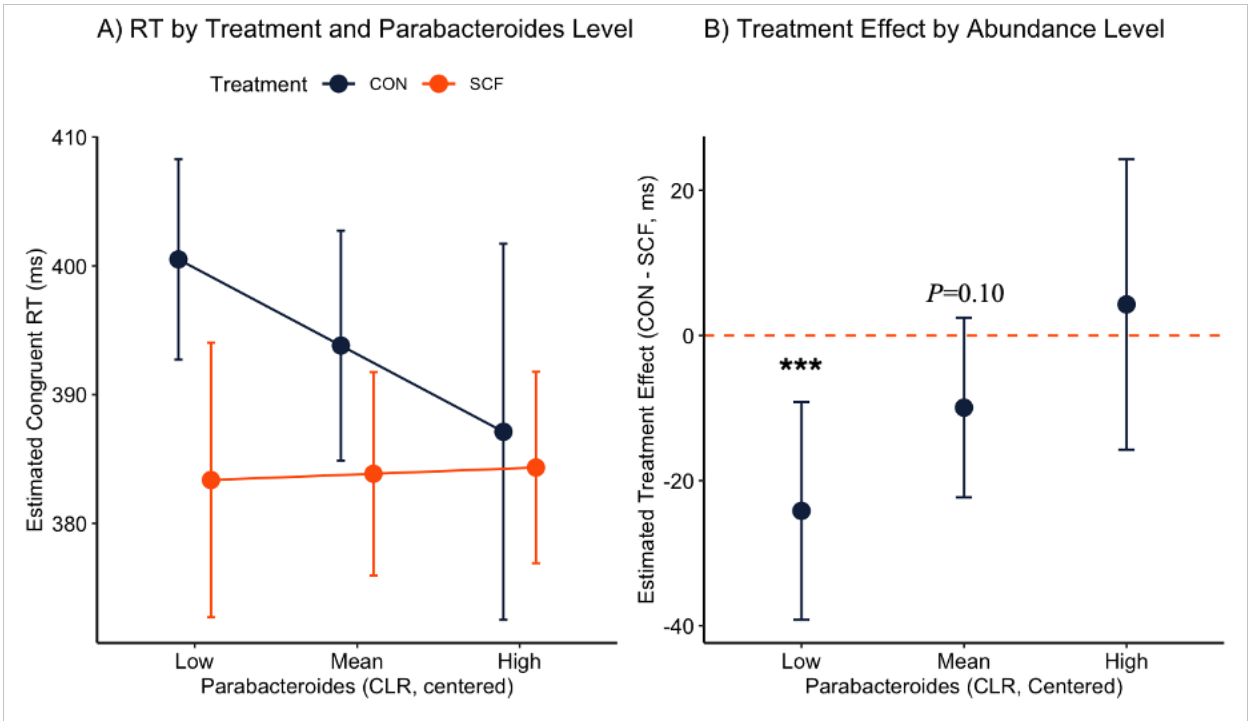

Figure 4. Moderation of the Treatment Effect on Congruent Reaction Time by Parabacteroides Abundance. Moderation model results illustrating the association between post-intervention Parabacteroides abundance (CLR-transformed, mean-centered) and the effect of treatment on congruent reaction time (RT) at endpoint (n = 37). Panel A) estimated marginal means and standard errors of estimated RT by treatment group at low (–1 SD), mean, and high (+1 SD) values of *Parabacteroides* abundance. Panel B) the estimated treatment effect (SCF – CON) on RT across the continuous range of *Parabacteroides* abundance, with 95% confidence intervals. The horizontal dashed line at zero represents no treatment effect. Estimates were derived from linear models described in the methods. Simple slopes and confidence intervals were generated using the Johnson-Neyman procedure, statistical significance is annotated as follows: ***$P < 0.001$.

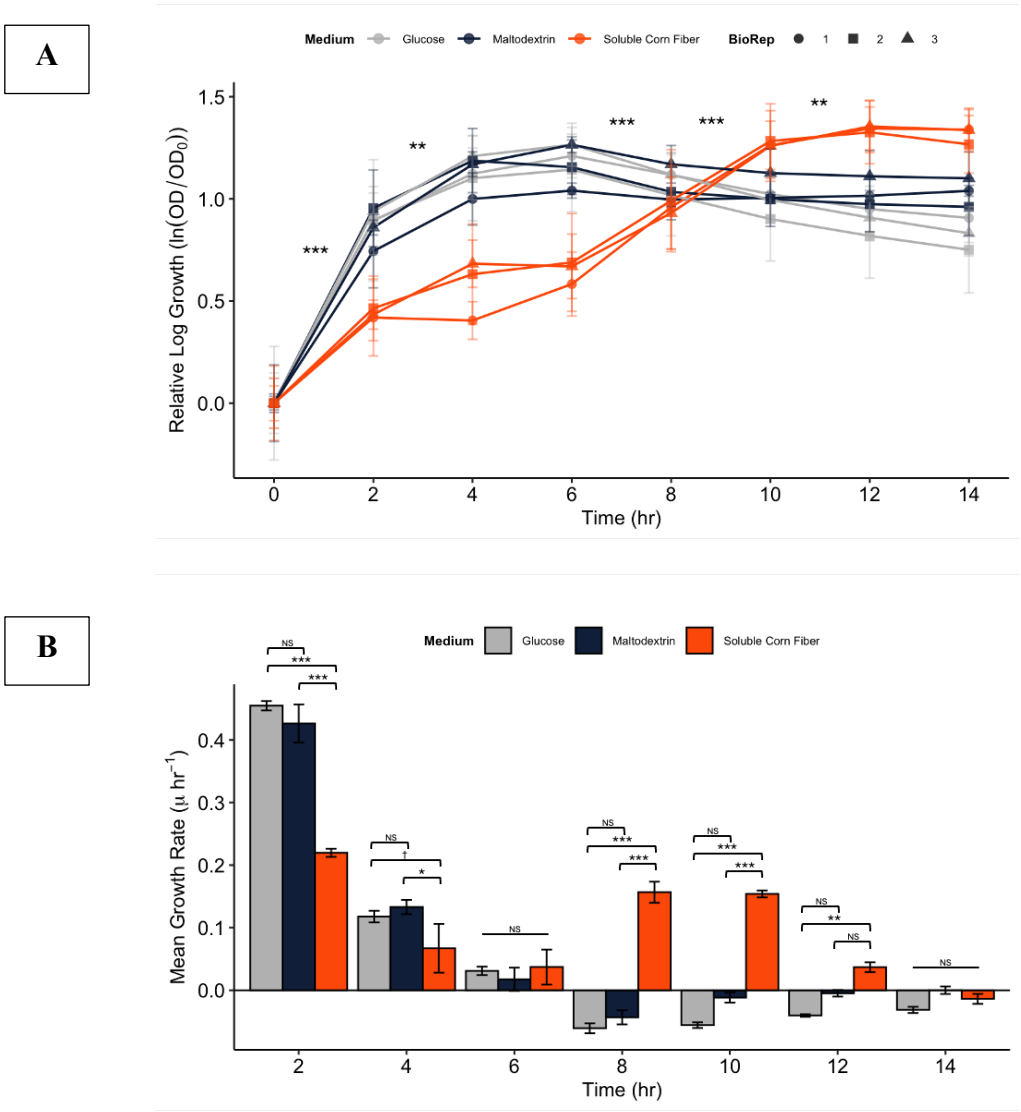

Figure 5. Growth Dynamics of *Parabacteroides distasonis* Cultures in M9 Medium Supplemented with Individual Carbohydrates. Panel A) Relative log growth (ln[OD/ OD_0]) of *P. distasonis* over time in M9 minimal medium supplemented with different carbohydrate sources. OD_0 represents the initial optical density (OD_{600}) at time zero. Each curve represents a mean biological replicate (N = 3), and error bars indicate propagated standard deviations. Panel B) Mean growth rate (μ, hr^{-1}), calculated as the slope of ln(OD) over sequential 2-hour intervals.

Bars represent average growth rate across replicates. Significance levels: †P < 0.1, *P < 0.05, **P < 0.01, ***P < 0.001, NS = not significant.

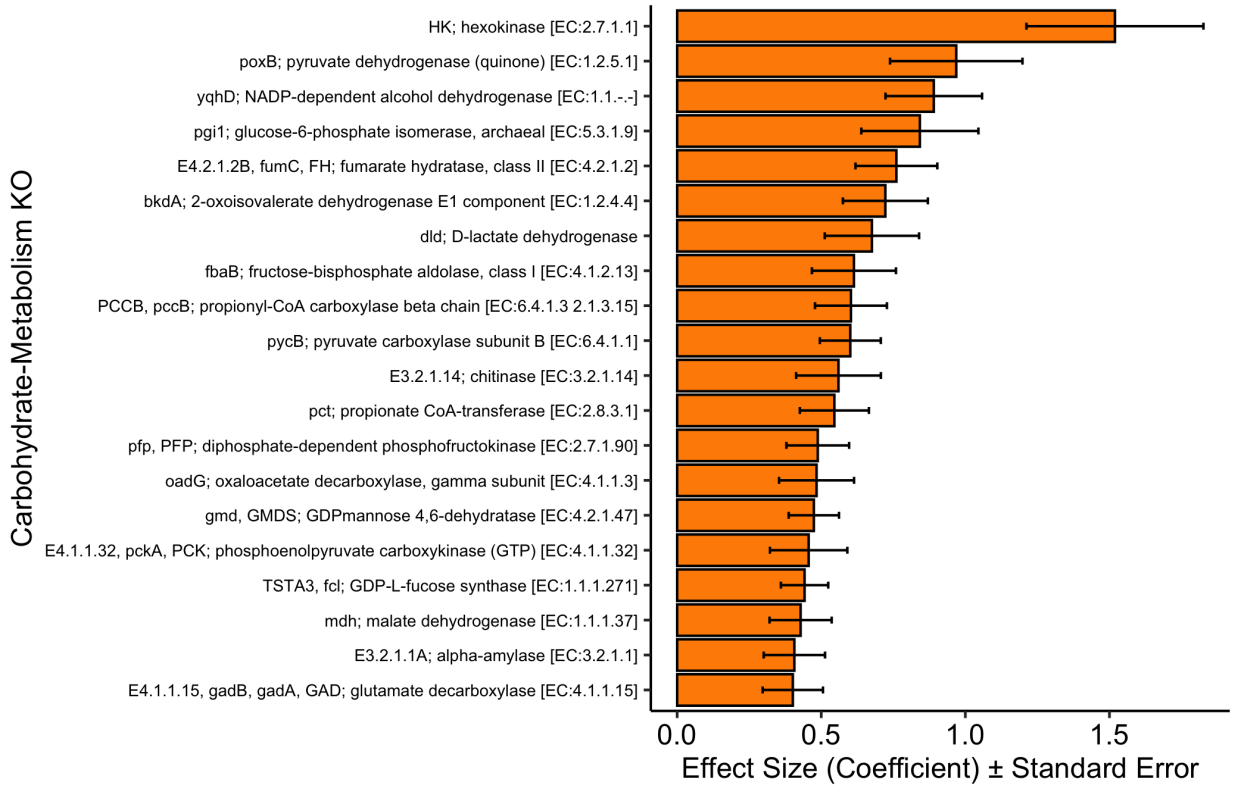

Figure 6. Differential Abundance of Predicted Carbohydrate Metabolism KOs at Endpoint Between Treatment. PICRUSt2-predicted KEGG Orthologs (KOs) related to carbohydrate metabolism with positive MaAsLin2 coefficients at post-intervention (POST) are shown (N = 39). Each bar represents the effect size (coefficient) and standard error estimating the direction and magnitude of the association between soluble corn fiber (SCF) treatment and KO abundance relative to control. Positive coefficients indicate higher predicted abundance in the SCF group; larger absolute values reflect stronger associations.

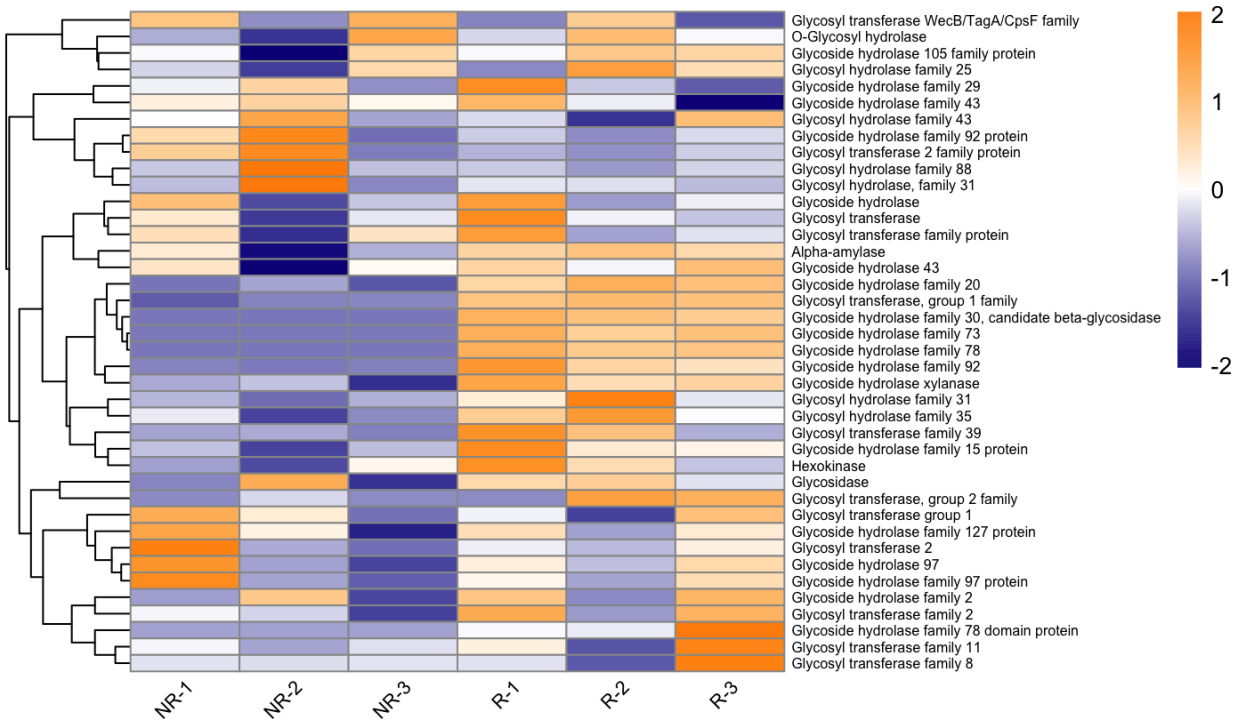

Figure 7. Differential Abundance of Carbohydrate Metabolism-Associated Genes Between Responders and Non-Responders to Soluble Corn Fiber Intervention. Heatmap displaying the abundance of carbohydrate metabolism-related gene families annotated by HUMAnN 3.0 across six participants (N = 6), stratified by responder (R1–R3) and non-responder (NR1–NR3) status. Genes families shown (rows) were selected from a total of 1,180 unique carbohydrate-associated gene families based on a $\log_2$ fold change > 2 in mean abundance between responders and non-responders [log2(R/NR)]. The top 40 gene families are presented. Abundance values were row-scaled using Z-score normalization to emphasize relative variation across samples. Orange indicates higher abundance, and blue indicates lower abundance for each gene.

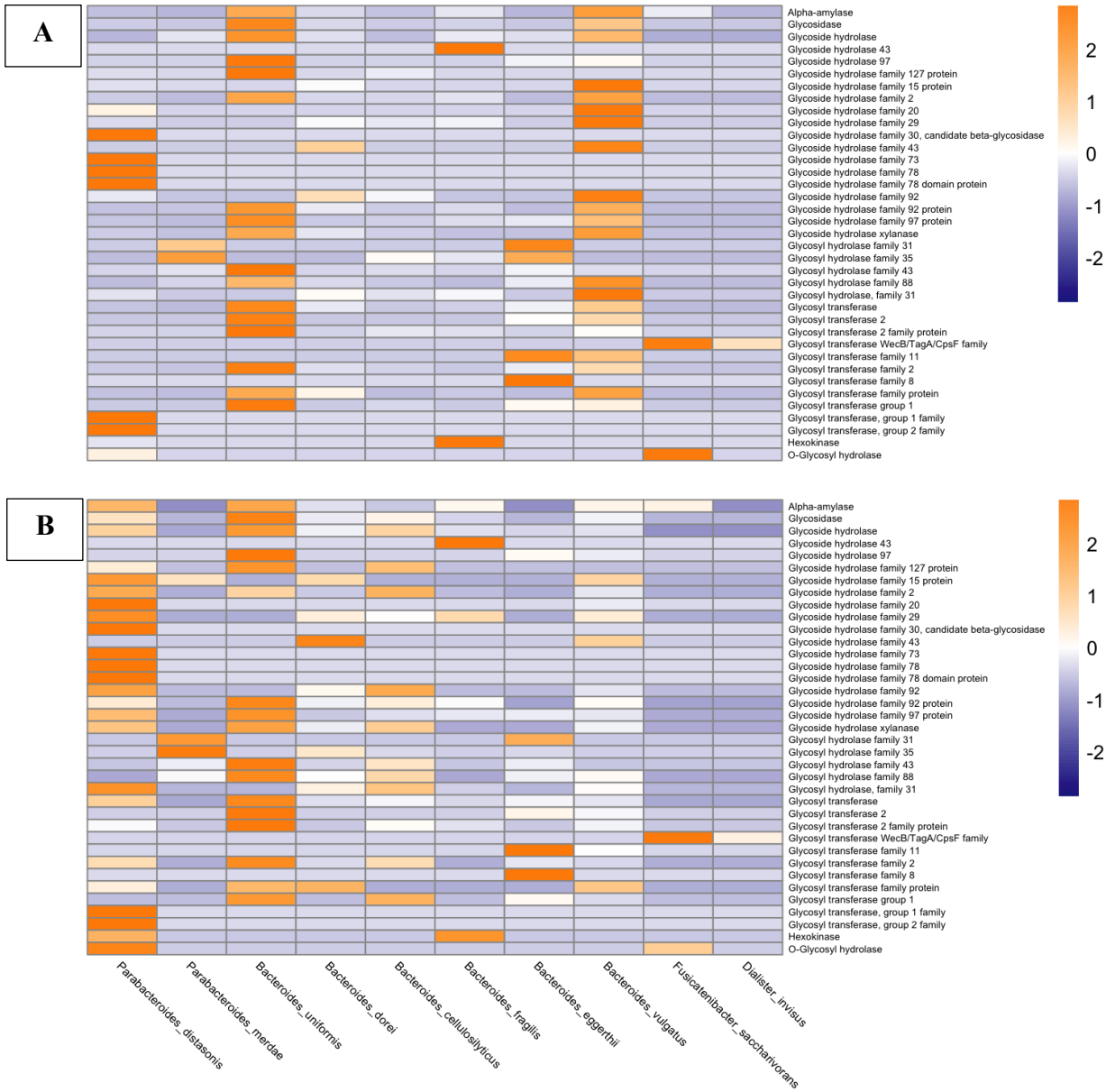

Figure 8. Species-Level Contributions to Carbohydrate Metabolism Gene Abundance Before and After Soluble Corn Fiber Intervention. Heatmaps showing the contribution of individual species (columns) to the abundance of 40 carbohydrate metabolism-associated gene families (rows) in six participants (N = 6). Panel A) before the SCF intervention, Panel B) after the SCF intervention. Gene abundance was row-normalized using Z-scores to highlight species-level contributions, with orange indicating higher and blue indicating lower abundance for each gene.